

# Towards hydrogen and halogen bonded frameworks based on 3,5-bis(triazolyl)pyridinium motifs

Émer M. Foyle, Hui Min Tay, and Nicholas G. White\*

*Research School of Chemistry, The Australian National University*

*137 Sullivan's Creek Road, Acton, 2600, ACT, Australia*

*Email: [nicholas.white@anu.edu.au](mailto:nicholas.white@anu.edu.au)*

*URL: [www.nwhitegroup.com](http://www.nwhitegroup.com)*

<b>Synthesis and characterization</b>	<b>2</b>
Details of instrumentation	2
Characterisation data for new compounds	3
Optimized synthesis of 3,5-diethynylpyridine	23
Synthesis of selenium containing receptors	24
<b>X-ray crystallography</b>	<b>30</b>
Details of data collection and refinement	30
Details of individual refinements	31
Table of crystallographic data	38
<b>Cambridge Structural Database (CSD) searches</b>	<b>39</b>
<b>References</b>	<b>40</b>

# Synthesis and characterization

## *Details of instrumentation*

NMR spectra were collected on Bruker Avance 400, 600 or 700 spectrometers and are referenced to the residual solvent signal.<sup>S1</sup> Electrospray ionisation mass spectrometry data were acquired on a Micromass Waters ZMD spectrometer. Details of X-ray crystallography are provided in a separate section.

## Characterization data for new compounds

Spectra for  $1^{\text{H}}_{\text{Bn}}$ :

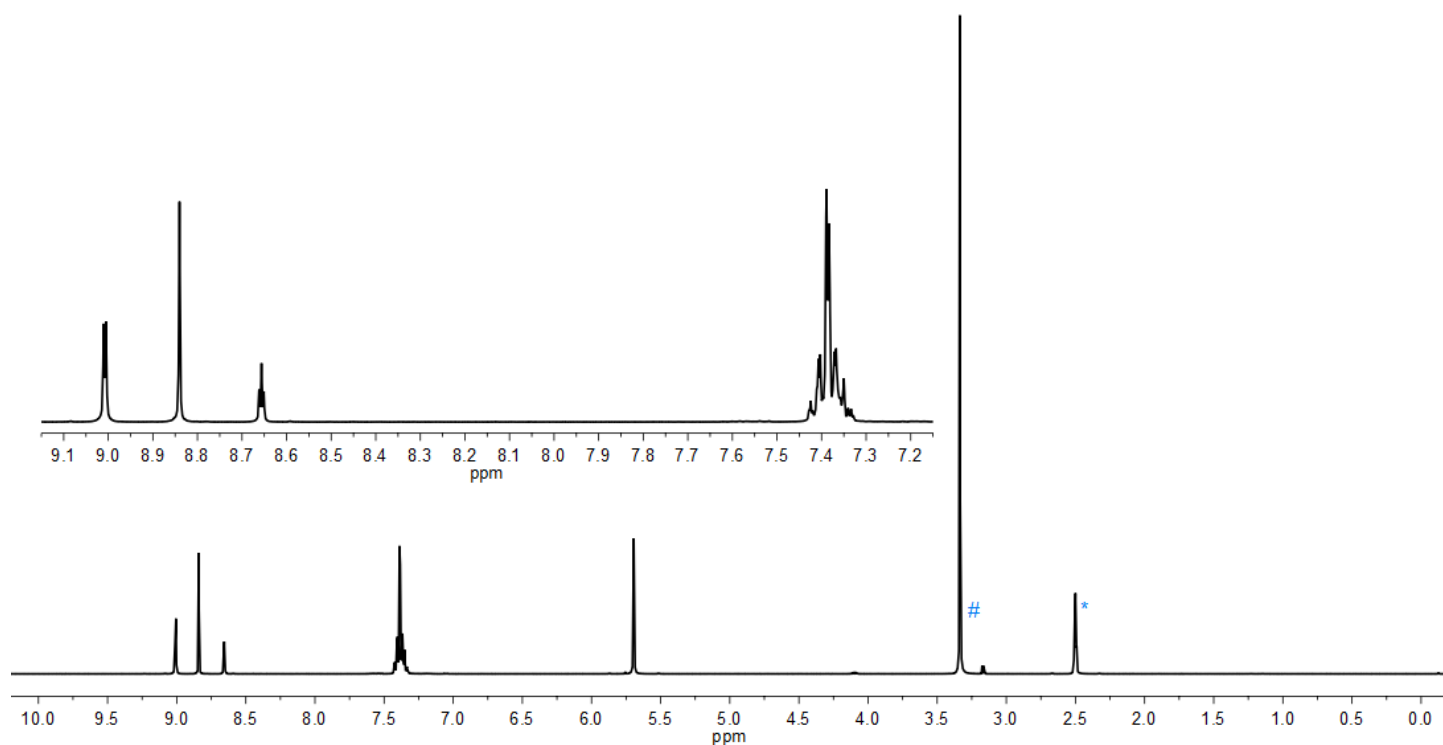


**Figure S1.**  $^1\text{H}$  NMR spectrum of  $1^{\text{H}}_{\text{Bn}}$ , peak labelled \* results from incompletely deuterated NMR solvent, peak labelled # results from water ( $\text{d}_6$ -DMSO, 400 MHz, 298 K).

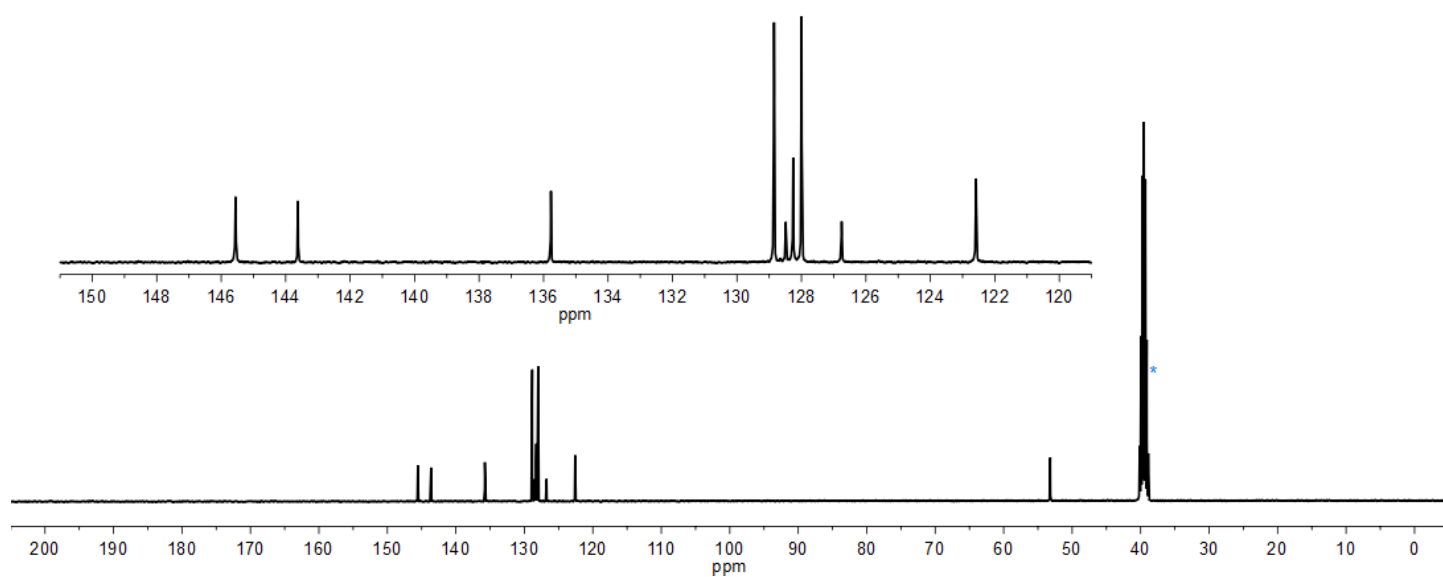


**Figure S2.**  $^{13}\text{C}$  NMR spectrum of  $1^{\text{H}}_{\text{Bn}}$ , peak labelled \* results from incompletely deuterated NMR solvent ( $\text{d}_6$ -DMSO, 101 MHz, 298 K).

Spectra for  $2^{\text{H}}_{\text{Hex}}\text{-Br}_2$ :

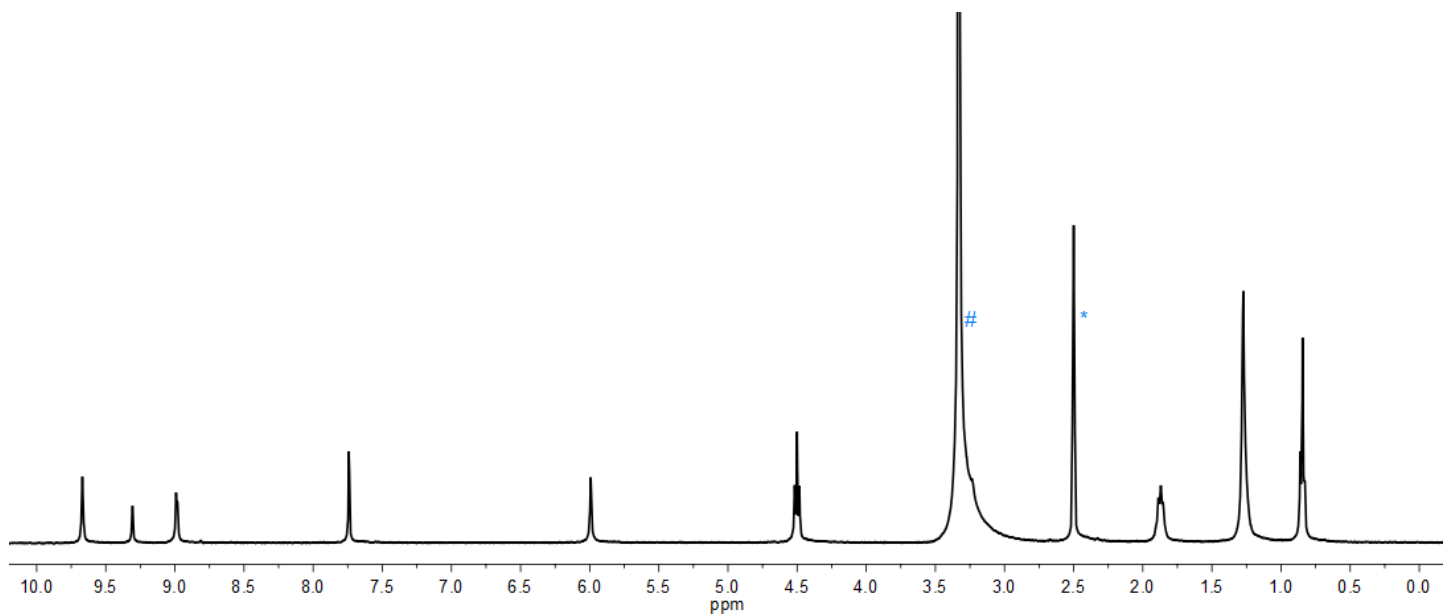


**Figure S3.**  $^1\text{H}$  NMR spectrum of  $2^{\text{H}}_{\text{Hex}}\text{-Br}_2$ , peak labelled \* results from incompletely deuterated NMR solvent, peak labelled # results from water and has been truncated ( $d_6$ -DMSO, 400 MHz, 298 K).

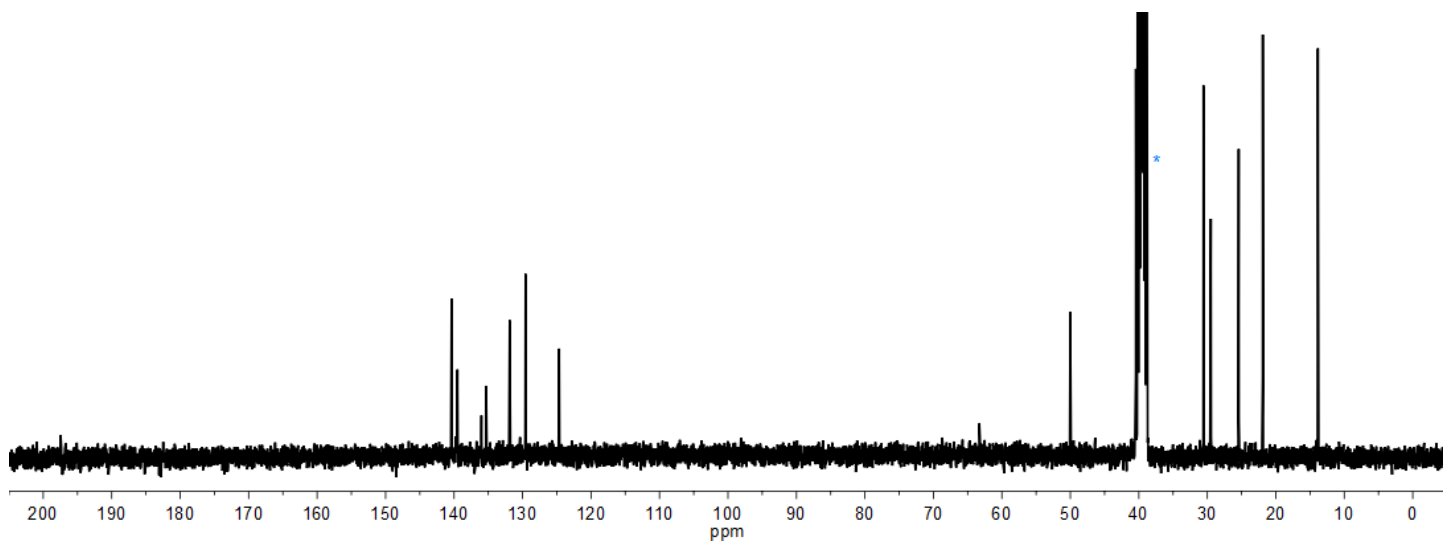


**Figure S4.**  $^{13}\text{C}$  NMR spectrum of  $2^{\text{H}}_{\text{Hex}}\text{-Br}_2$ , peak labelled \* results from incompletely deuterated NMR solvent and has been truncated ( $d_6$ -DMSO, 101 MHz, 298 K).

Spectra for  $2^{\text{H}}_{\text{Hex}}(\text{PF}_6)_2$ :

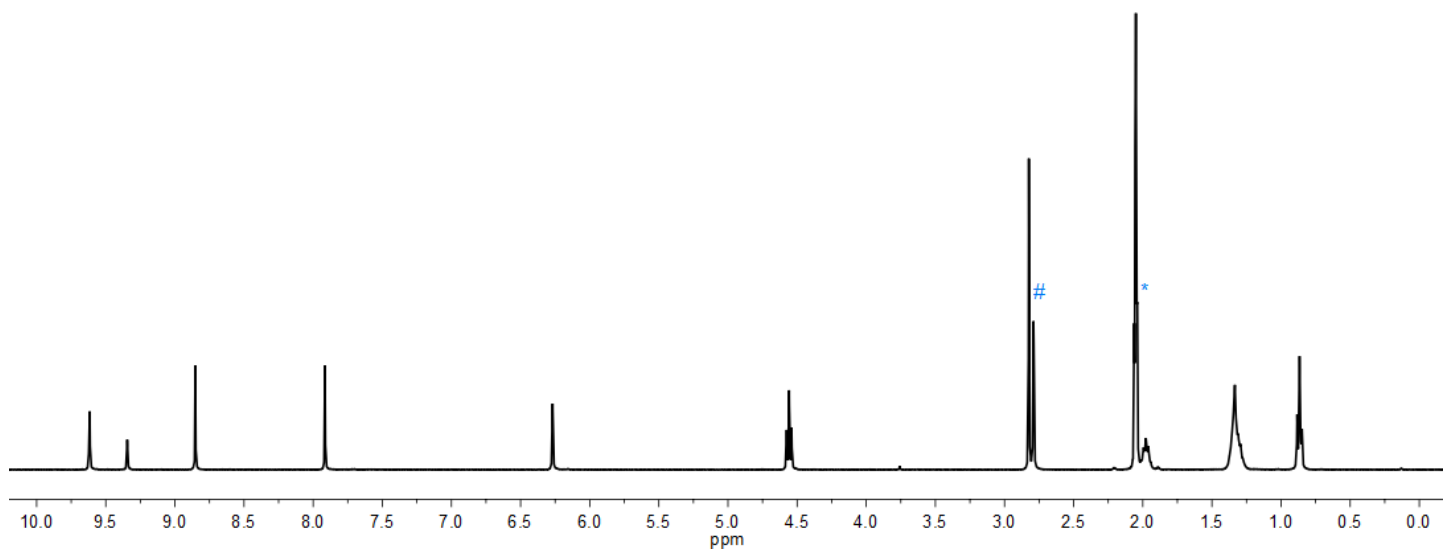


**Figure S5.**  $^1\text{H}$  NMR spectrum of  $2^{\text{H}}_{\text{Hex}}(\text{PF}_6)_2$ , peak labelled \* results from incompletely deuterated NMR solvent, peak labelled # results from water ( $\text{d}_6$ -acetone, 400 MHz, 298 K).

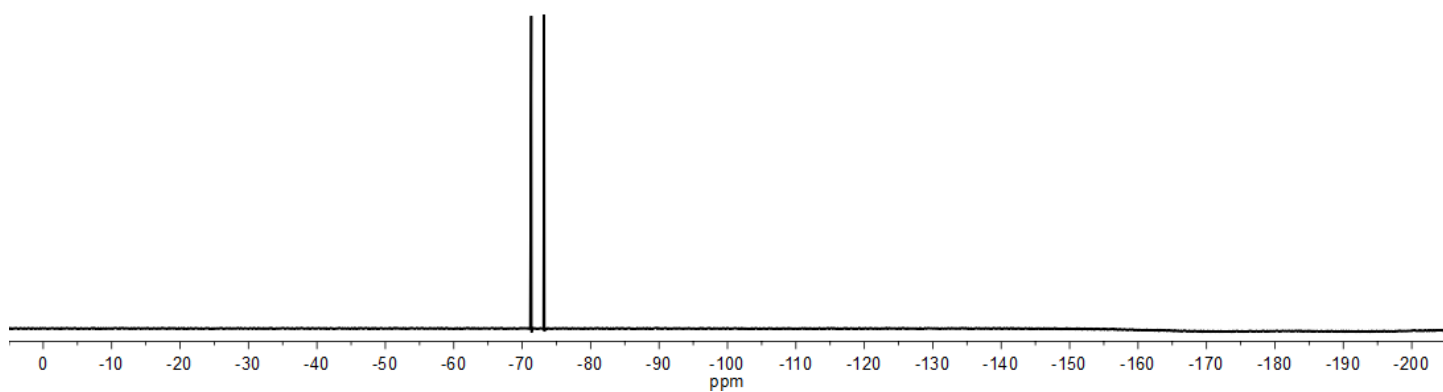


**Figure S6.**  $^{19}\text{F}$  NMR spectrum of  $2^{\text{H}}_{\text{Hex}}(\text{PF}_6)_2$ , ( $\text{d}_6$ -acetone, 376 MHz, 298 K).

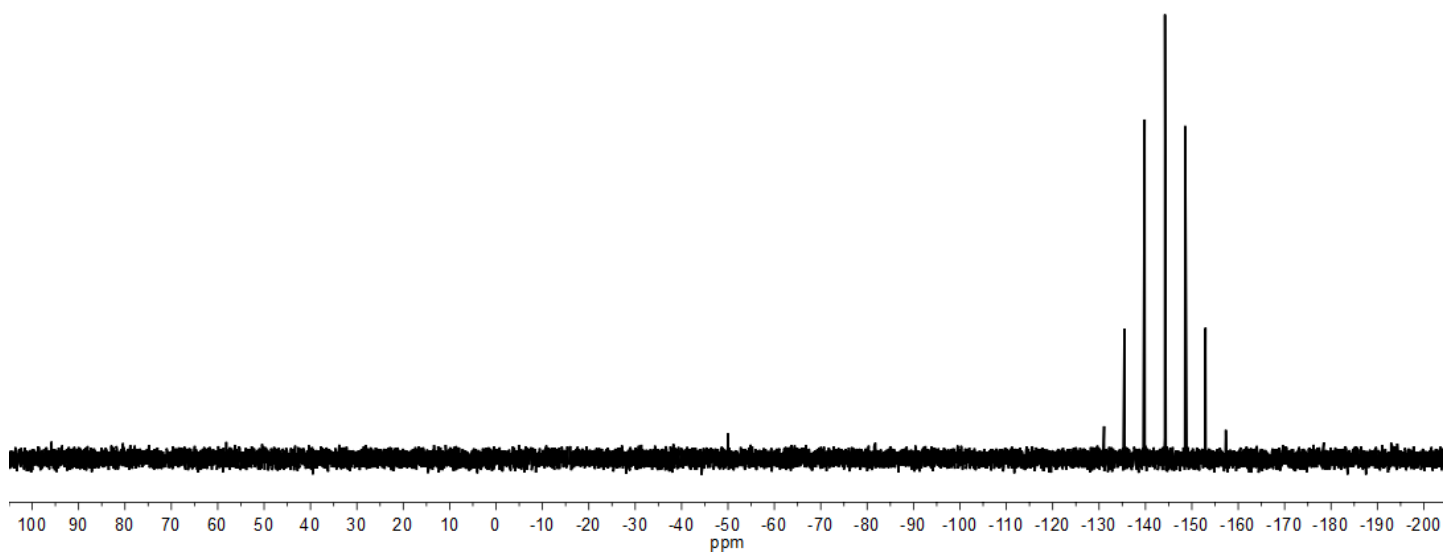


**Figure S7.**  $^{31}\text{P}$  NMR spectrum of  $2^{\text{H}}_{\text{Hex}}(\text{PF}_6)_2$ , ( $\text{d}_6$ -acetone, 162 MHz, 298 K).

Spectra for  $2^{\text{H}}_{\text{Bn}}\cdot\text{Br}_2$ :

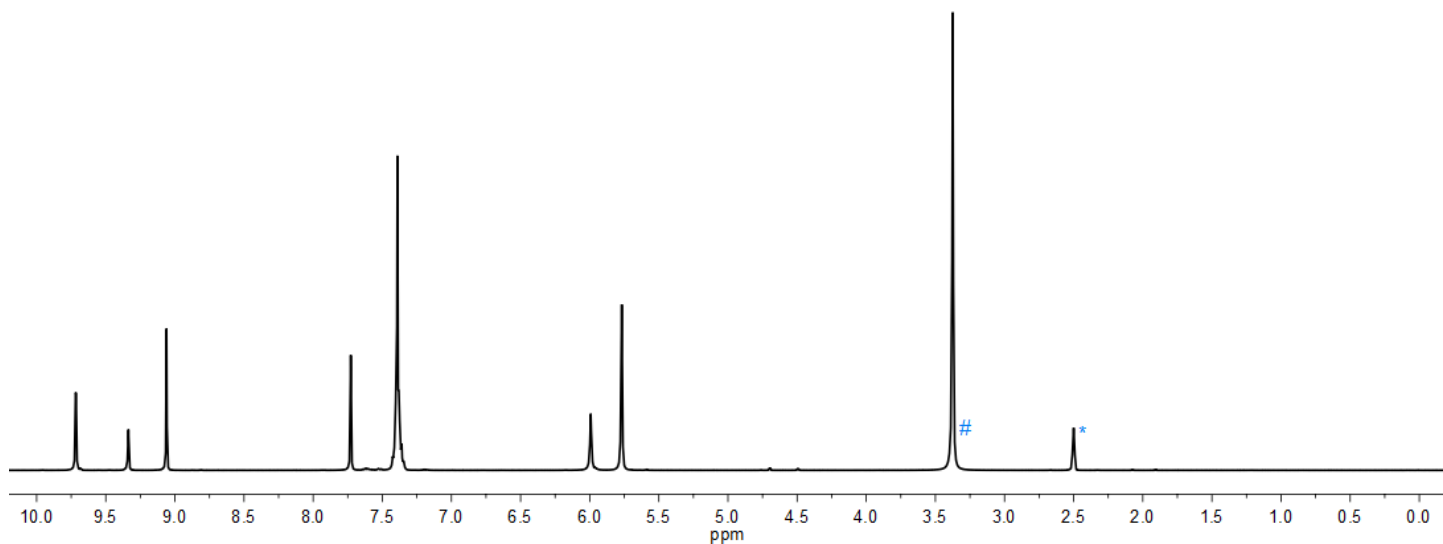


**Figure S8.**  $^1\text{H}$  NMR spectrum of  $2^{\text{H}}_{\text{Bn}}\cdot\text{Br}_2$ , peak labelled \* results from incompletely deuterated NMR solvent, peak labelled # results from water ( $\text{d}_6$ -DMSO, 400 MHz, 298 K).

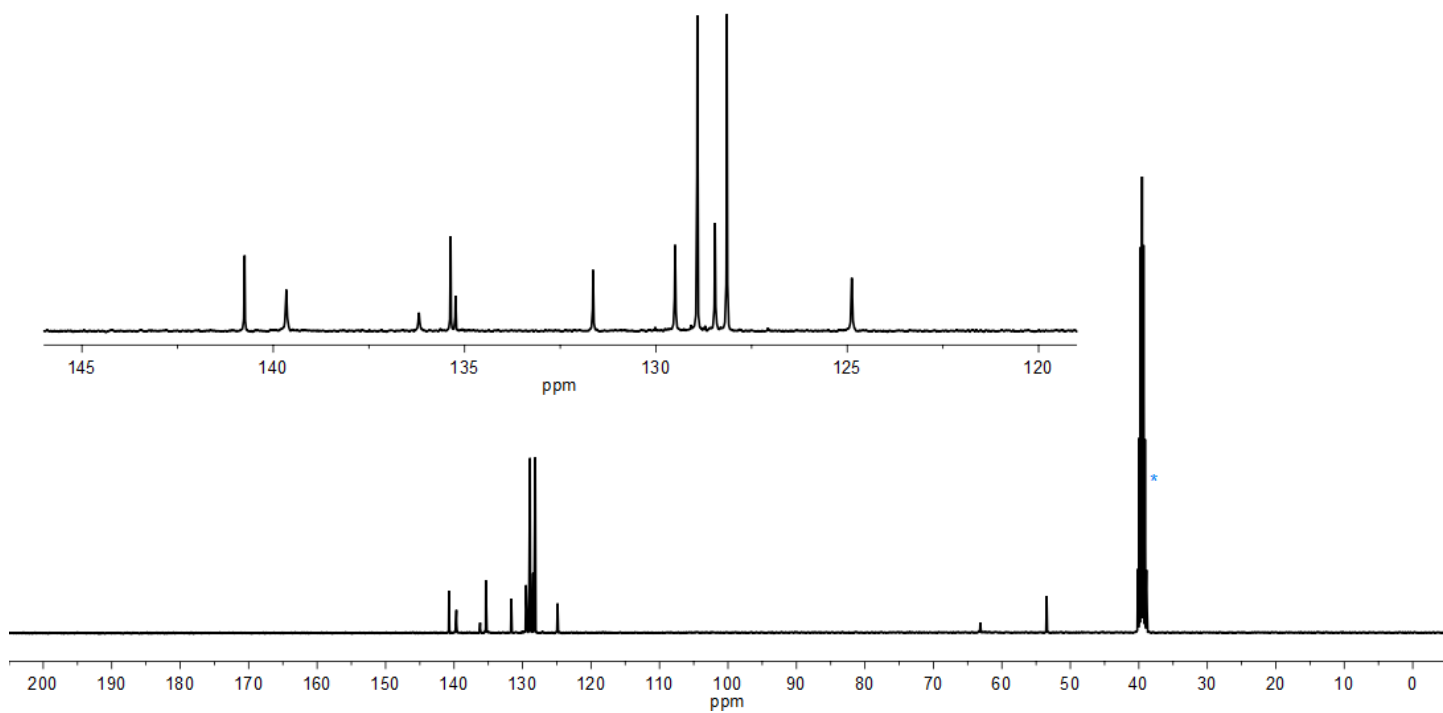


**Figure S9.**  $^{13}\text{C}$  NMR spectrum of  $2^{\text{H}}_{\text{Bn}}\cdot\text{Br}_2$ , peak labelled \* results from incompletely deuterated NMR solvent ( $\text{d}_6$ -DMSO, 101 MHz, 298 K).

Spectra for  $2^{\text{H}}_{\text{Bn}}(\text{PF}_6)_2$ :

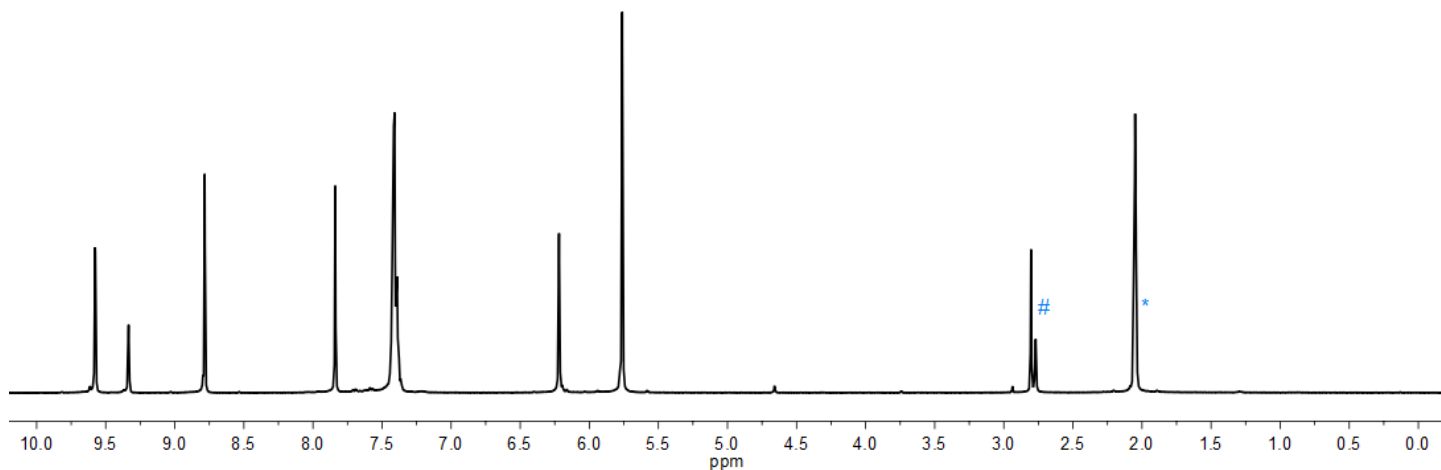


**Figure S10.**  $^1\text{H}$  NMR spectrum of  $2^{\text{H}}_{\text{Hex}}(\text{PF}_6)_2$ , peak labelled \* results from incompletely deuterated NMR solvent, peak labelled # results from water ( $\text{d}_6$ -acetone, 400 MHz, 298 K).

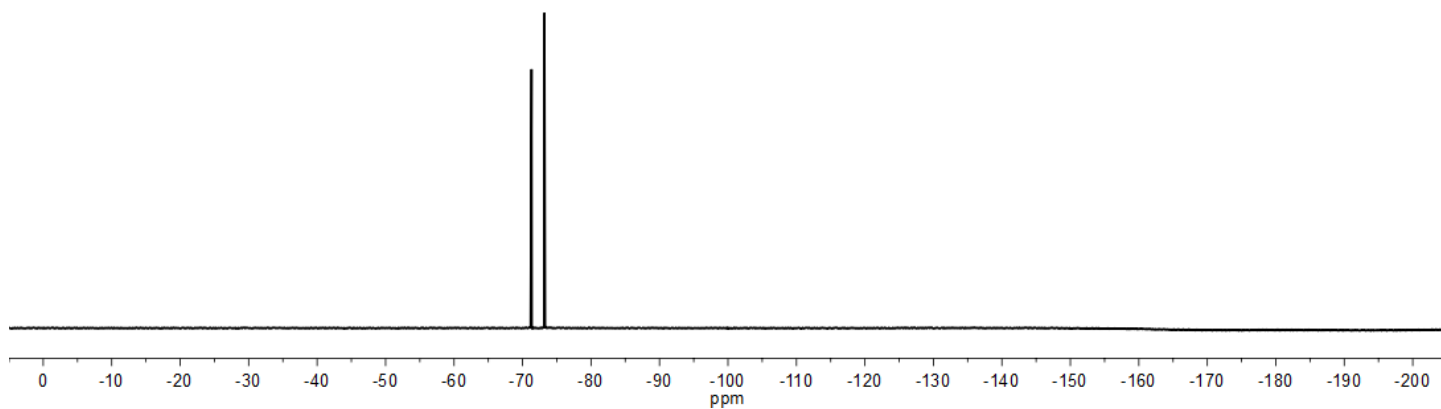


**Figure S11.**  $^{19}\text{F}$  NMR spectrum of  $2^{\text{H}}_{\text{Hex}}(\text{PF}_6)_2$  ( $\text{d}_6$ -acetone, 376 MHz, 298 K).

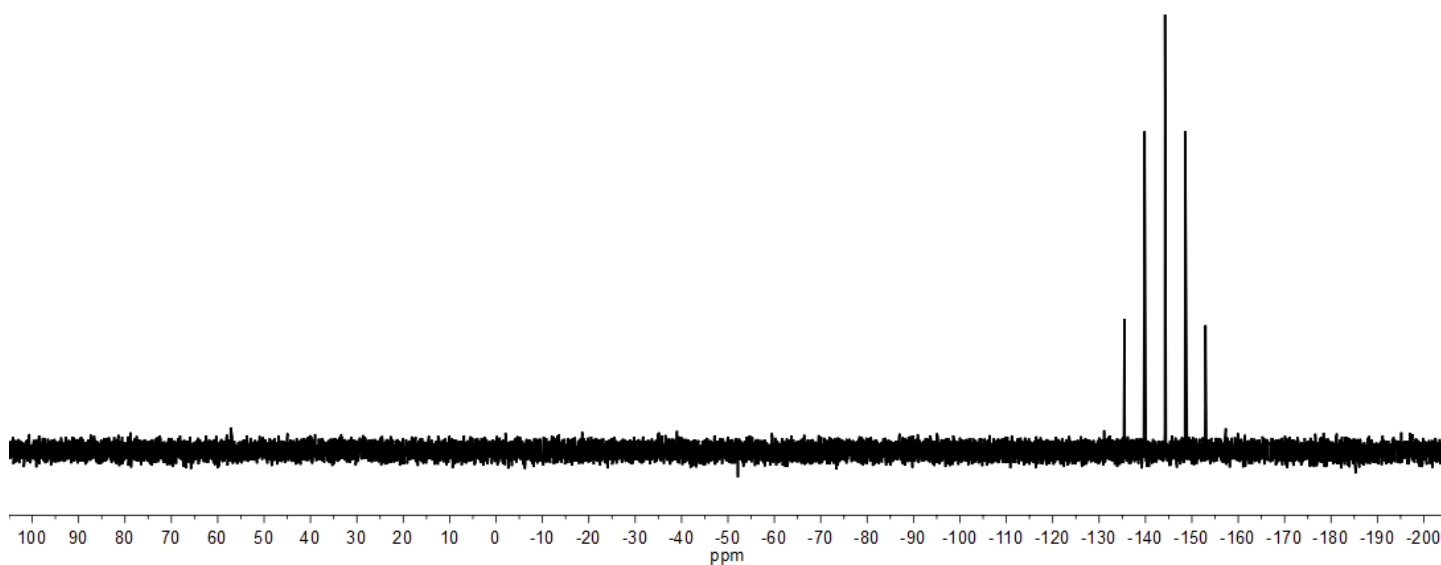


**Figure S12.**  $^{31}\text{P}$  NMR spectrum of  $2^{\text{H}}_{\text{Hex}}(\text{PF}_6)_2$  ( $\text{d}_6$ -acetone, 162 MHz, 298 K).

Spectra for  $2^1_{\text{Bn}}\text{-Br}_2$ :

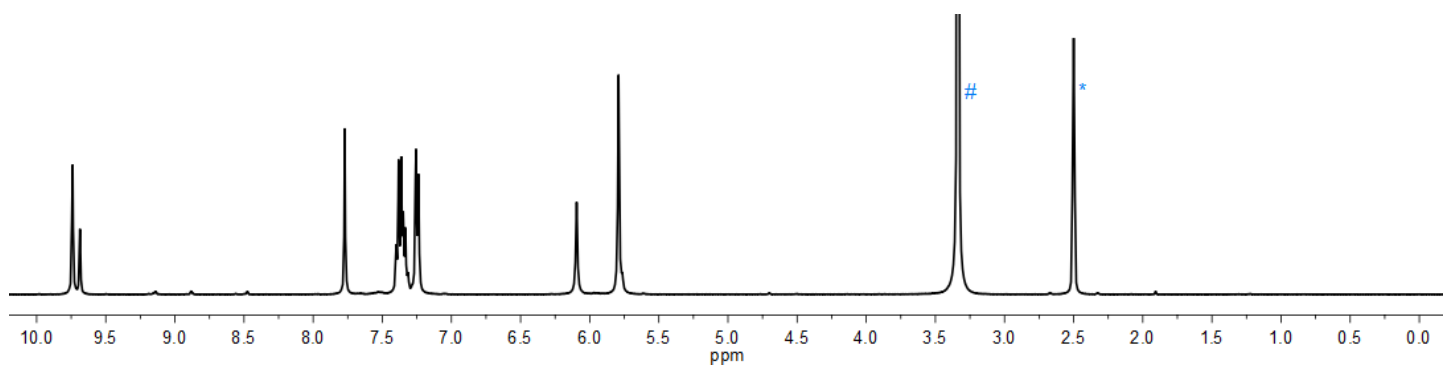


**Figure S13.**  $^1\text{H}$  NMR spectrum of  $2^1_{\text{Bn}}\text{-Br}_2$ , peak labelled \* results from incompletely deuterated NMR solvent, peak labelled # results from water and has been truncated ( $\text{d}_6\text{-DMSO}$ , 400 MHz, 298 K).

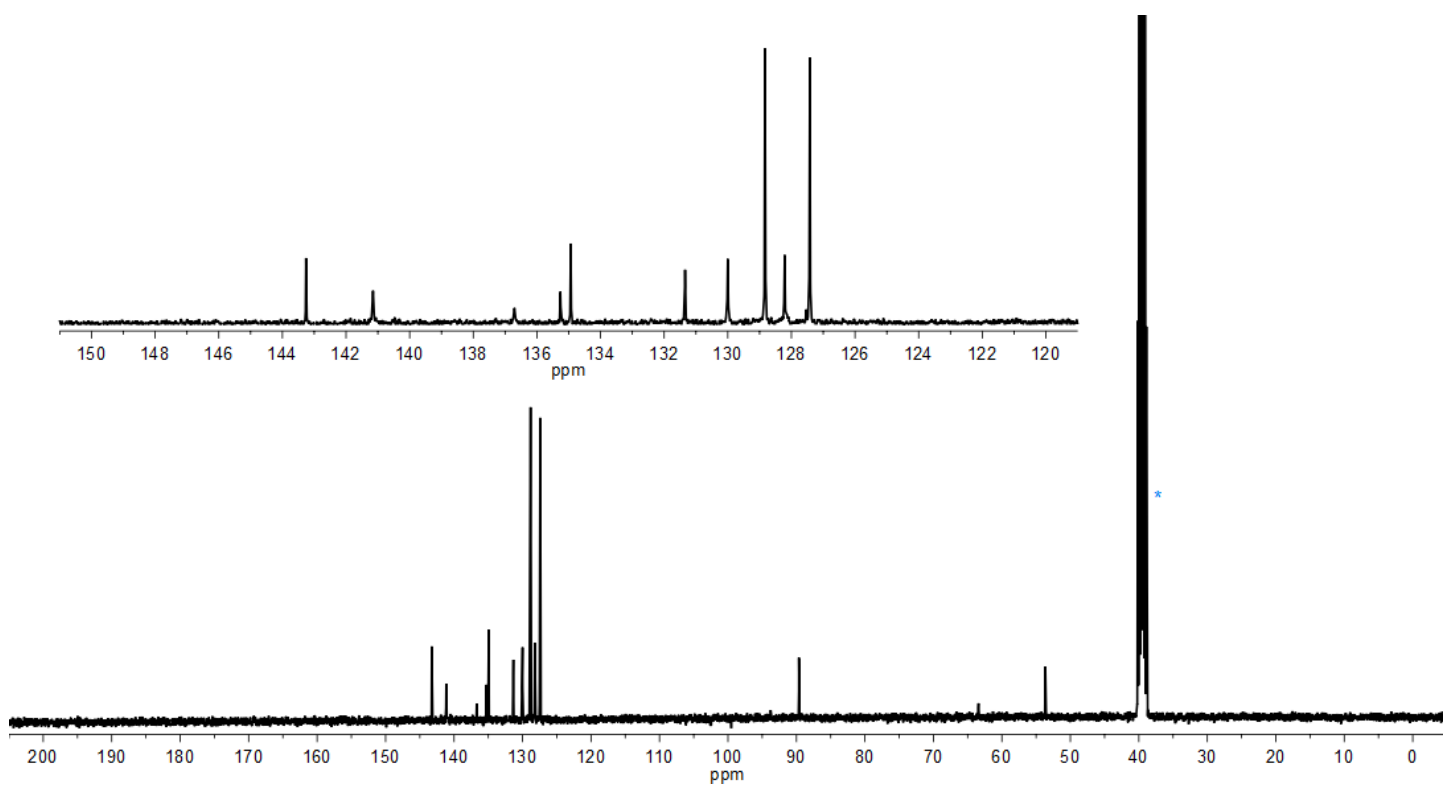


**Figure S14.**  $^{13}\text{C}$  NMR spectrum of  $2^1_{\text{Bn}}\text{-Br}_2$ , peak labelled \* results from incompletely deuterated NMR solvent and has been truncated ( $\text{d}_6\text{-DMSO}$ , 101 MHz, 298 K).

Spectra for  $2^1_{\text{Bn}}(\text{BF}_4)_2$ :

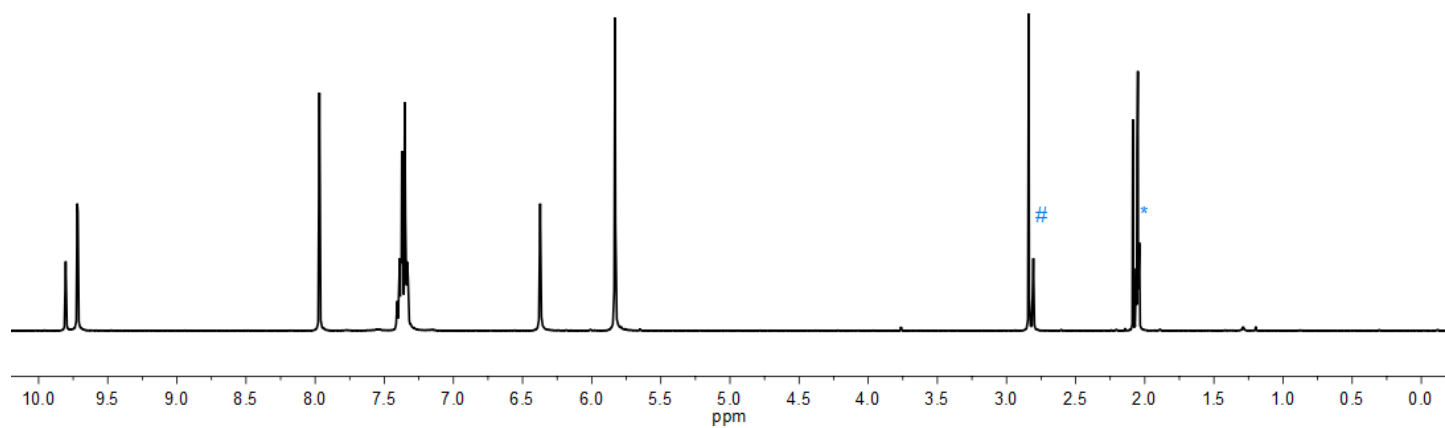


**Figure S15.**  $^1\text{H}$  NMR spectrum of  $2^1_{\text{Bn}}(\text{BF}_4)_2$ , peak labelled \* results from incompletely deuterated NMR solvent, peak labelled # results from water ( $d_6$ -acetone, 400 MHz, 298 K).

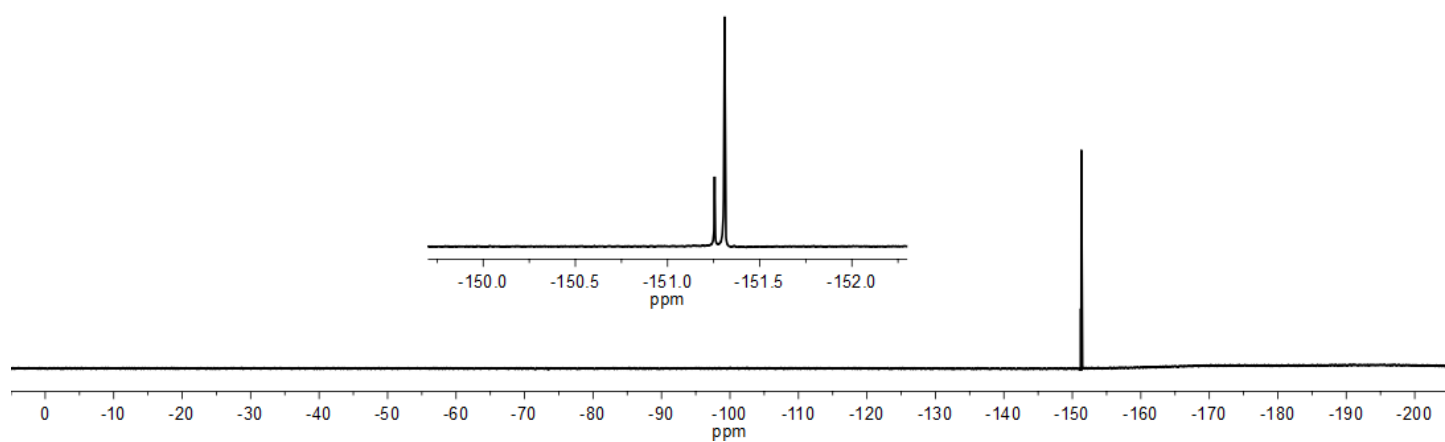


**Figure S16.**  $^{19}\text{F}$  NMR spectrum of  $2^1_{\text{Bn}}(\text{BF}_4)_2$  ( $d_6$ -acetone, 376 MHz, 298 K).

Spectra for 3:

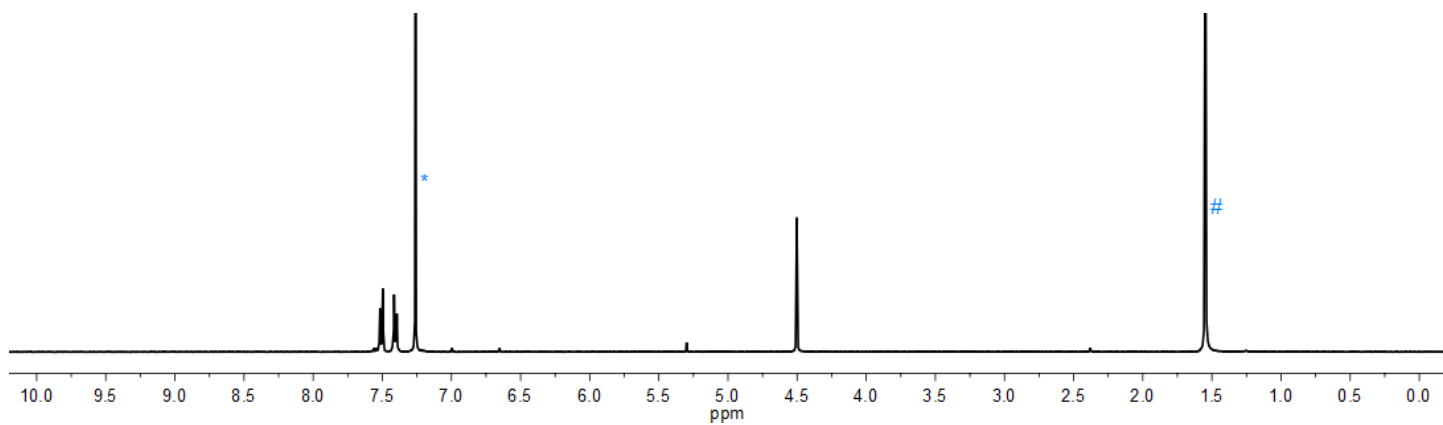


**Figure S17.**  $^1\text{H}$  NMR spectrum of **3**, peak labelled \* results from incompletely deuterated NMR solvent, peak labelled # results from water ( $\text{CDCl}_3$ , 400 MHz, 298 K).

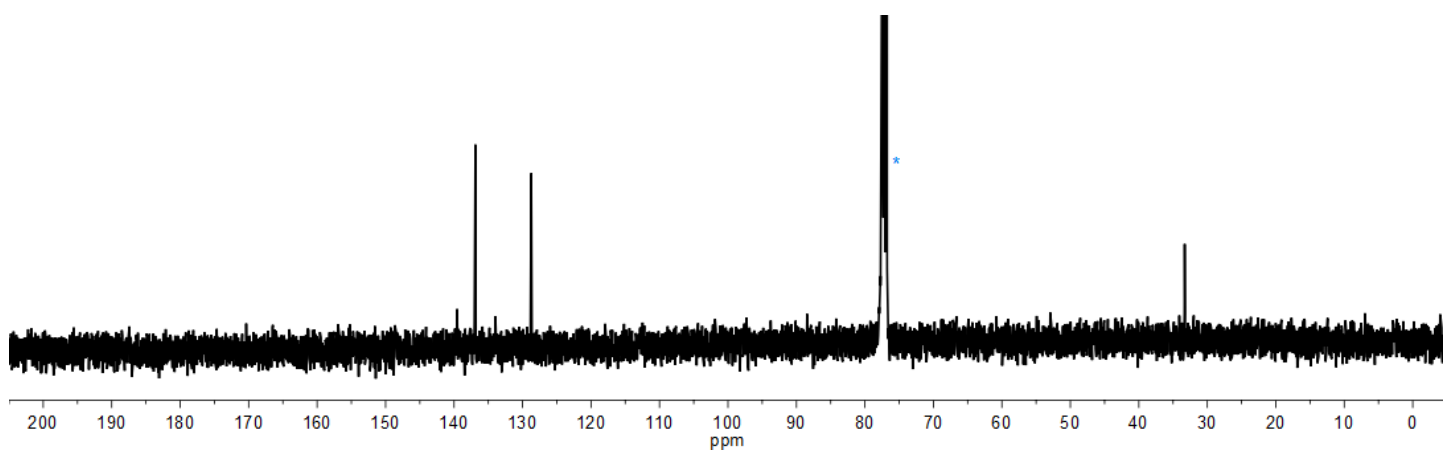


**Figure S18.**  $^{13}\text{C}$  NMR spectrum of **3**, peak labelled \* results from incompletely deuterated NMR solvent and has been truncated ( $\text{CDCl}_3$ , 101 MHz, 298 K).

Spectra for  $4^{\text{H}}\text{-Br}_4$ :

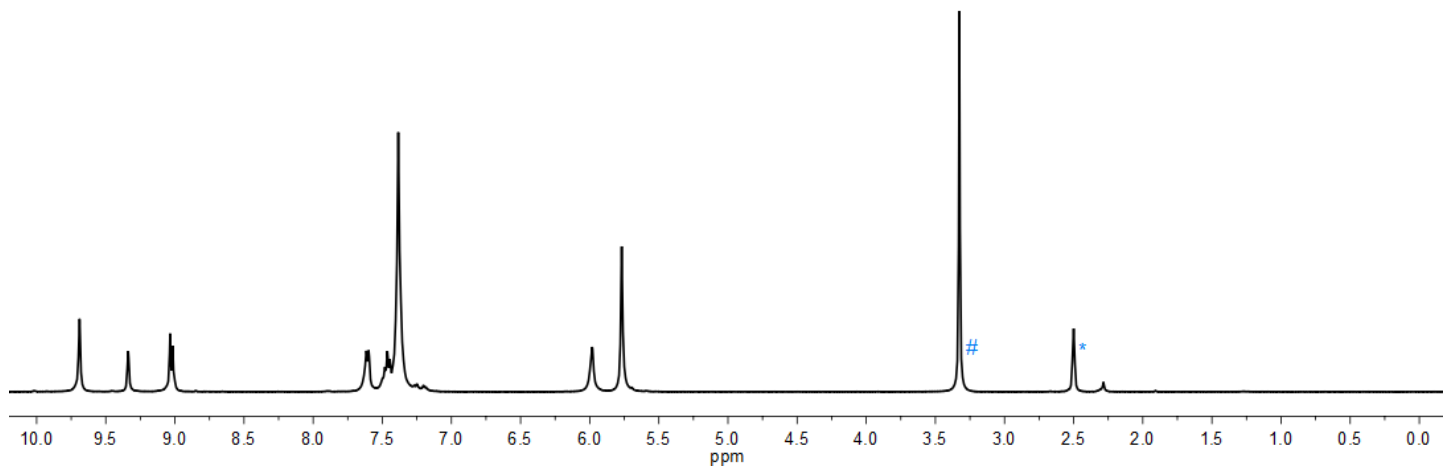


**Figure S19.**  $^1\text{H}$  NMR spectrum of  $4^{\text{H}}\text{-Br}_4$ , peak labelled \* results from incompletely deuterated NMR solvent, peak labelled # results from water ( $\text{d}_6\text{-DMSO}$ , 400 MHz, 298 K).

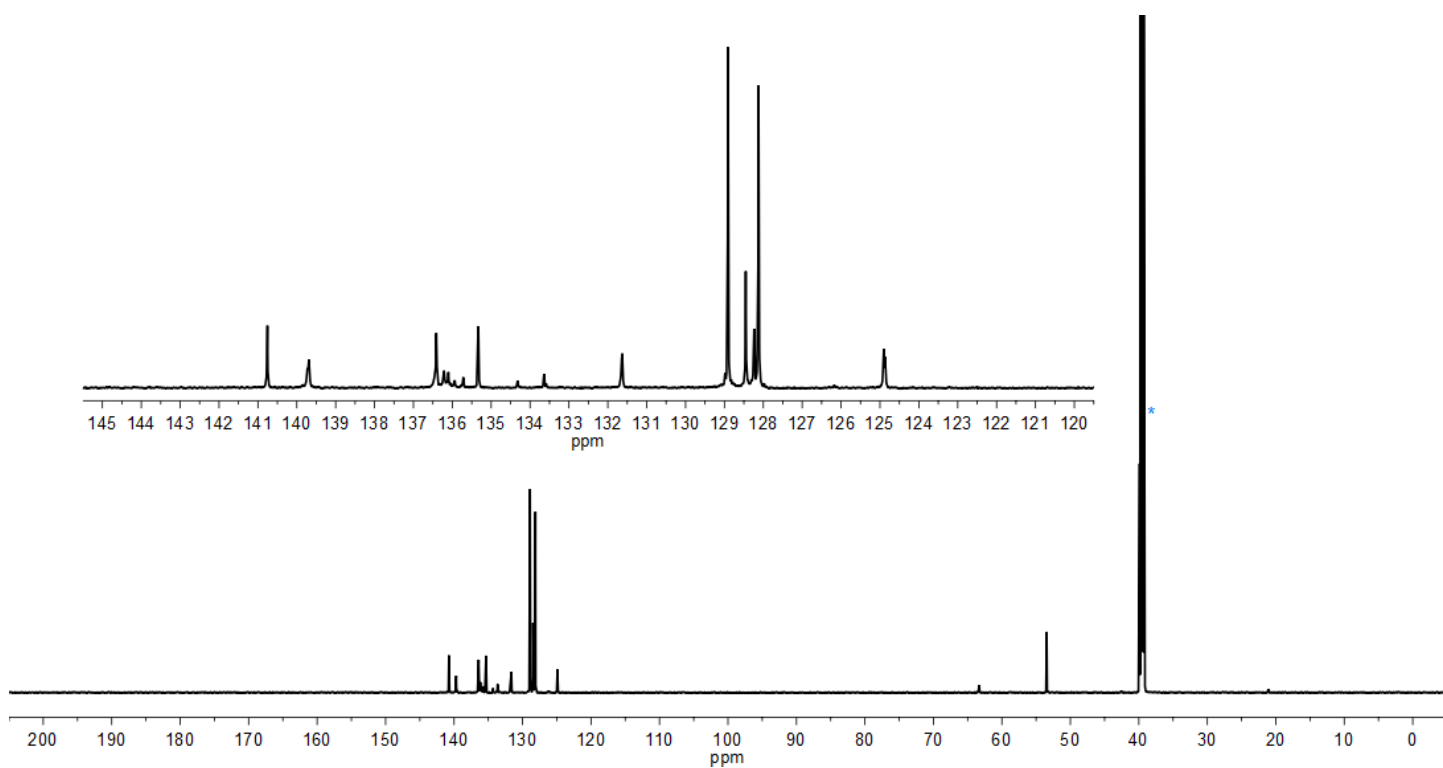


**Figure S20.**  $^{13}\text{C}$  NMR spectrum of  $4^{\text{H}}\text{-Br}_4$ , peak labelled \* results from incompletely deuterated NMR solvent and has been truncated ( $\text{d}_6\text{-DMSO}$ , 176 MHz, 298 K).

Spectra for  $4^{\text{H}}\text{-(PF}_6)_4$ :

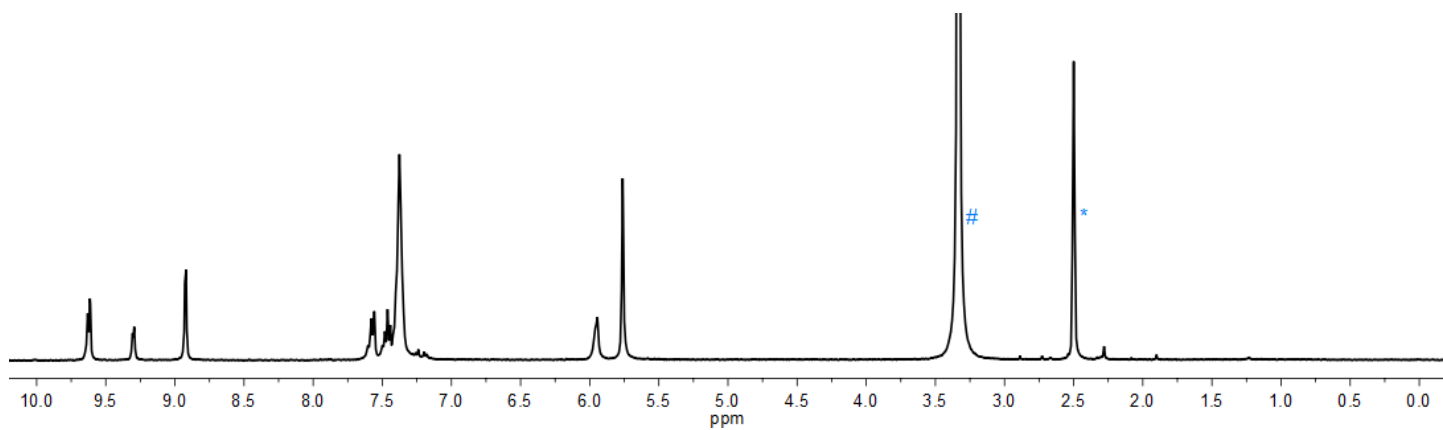


**Figure S21.**  $^1\text{H}$  NMR spectrum of  $4^{\text{H}}\text{-(PF}_6)_4$ , peak labelled \* results from incompletely deuterated NMR solvent, peak labelled # results from water and has been truncated ( $\text{d}_6\text{-DMSO}$ , 400 MHz, 298 K).

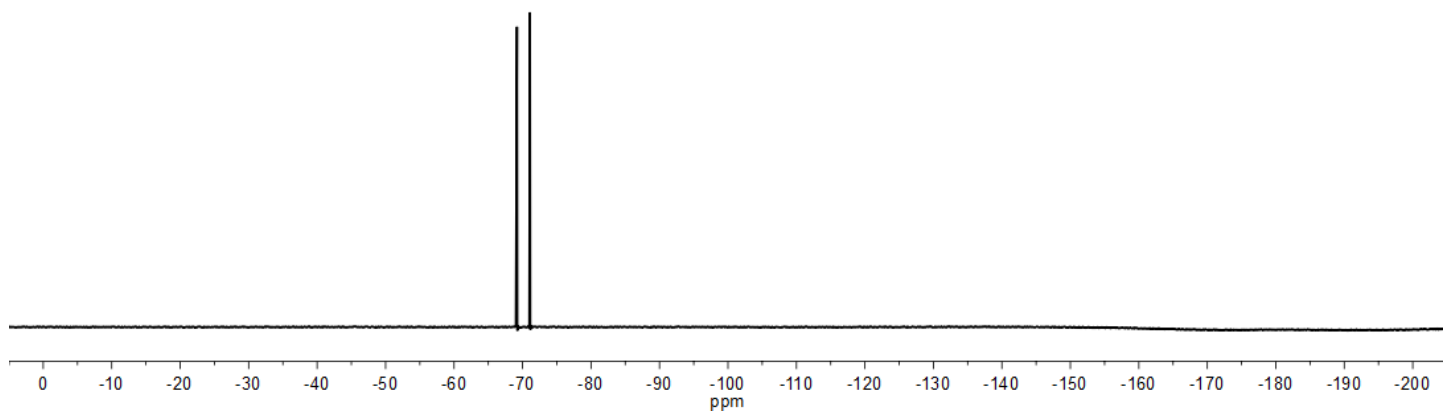


**Figure S22.**  $^{19}\text{F}$  NMR spectrum of  $4^{\text{H}}\text{-(PF}_6)_4$  ( $\text{d}_6\text{-DMSO}$ , 376 MHz, 298 K).

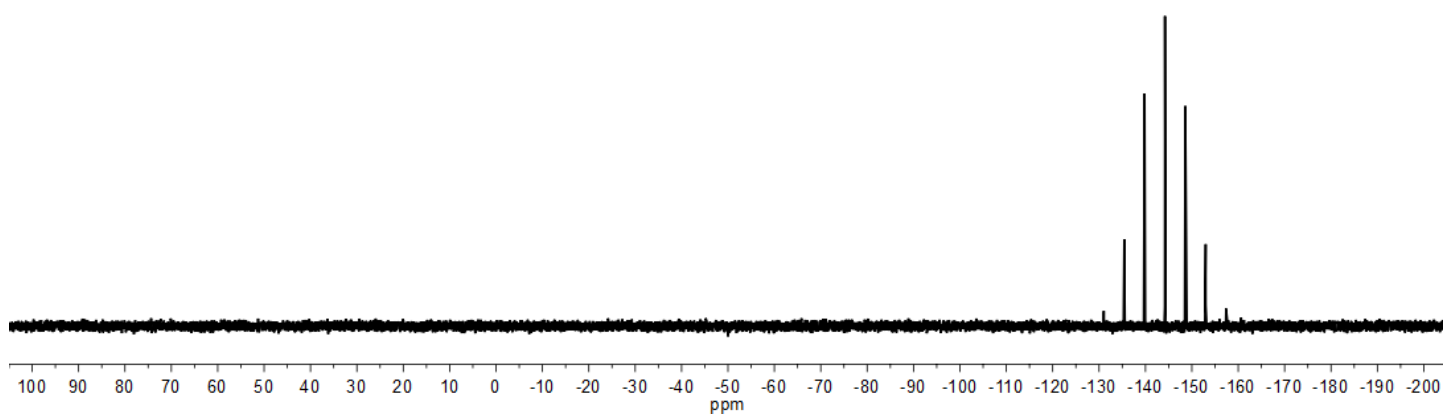


**Figure S23.**  $^{31}\text{P}$  NMR spectrum of  $4^{\text{H}}\text{-(PF}_6)_4$  ( $\text{d}_6\text{-DMSO}$ , 162 MHz, 298 K).

## Spectra for $4^1\text{-Br}_4$ :

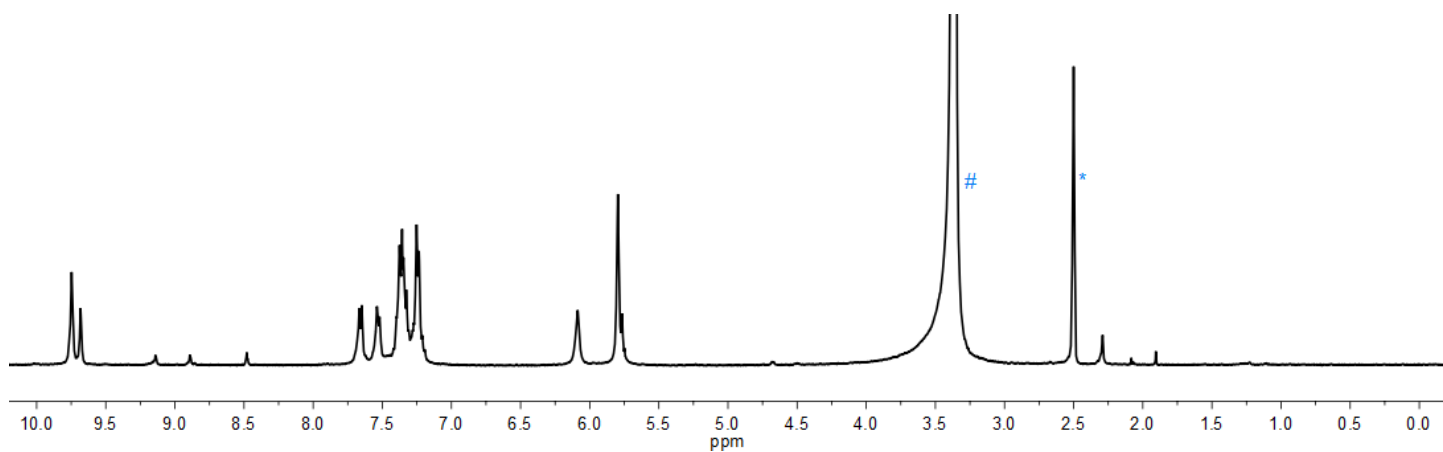


**Figure S24.**  $^1\text{H}$  NMR spectrum of  $4^1\text{-Br}_4$ , peak labelled \* results from incompletely deuterated NMR solvent, peak labelled # results from water and has been truncated ( $\text{d}_6\text{-DMSO}$ , 400 MHz, 298 K).

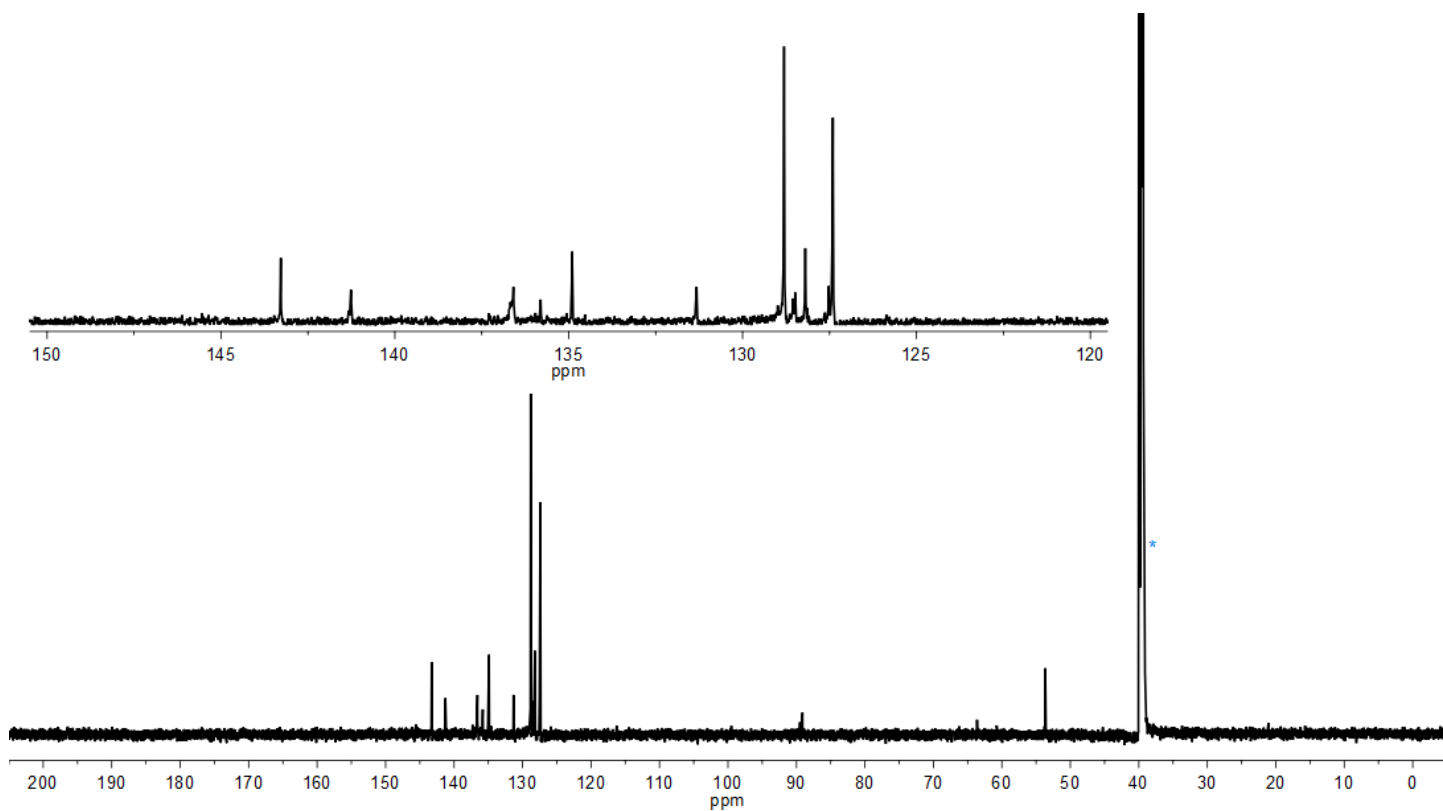


**Figure S25.**  $^{13}\text{C}$  NMR spectrum of  $4^1\text{-Br}_4$ , peak labelled \* results from incompletely deuterated NMR solvent and has been truncated ( $\text{d}_6\text{-DMSO}$ , 176 MHz, 298 K).

Spectra for  $4^1\text{-(BF}_4)_4$ :

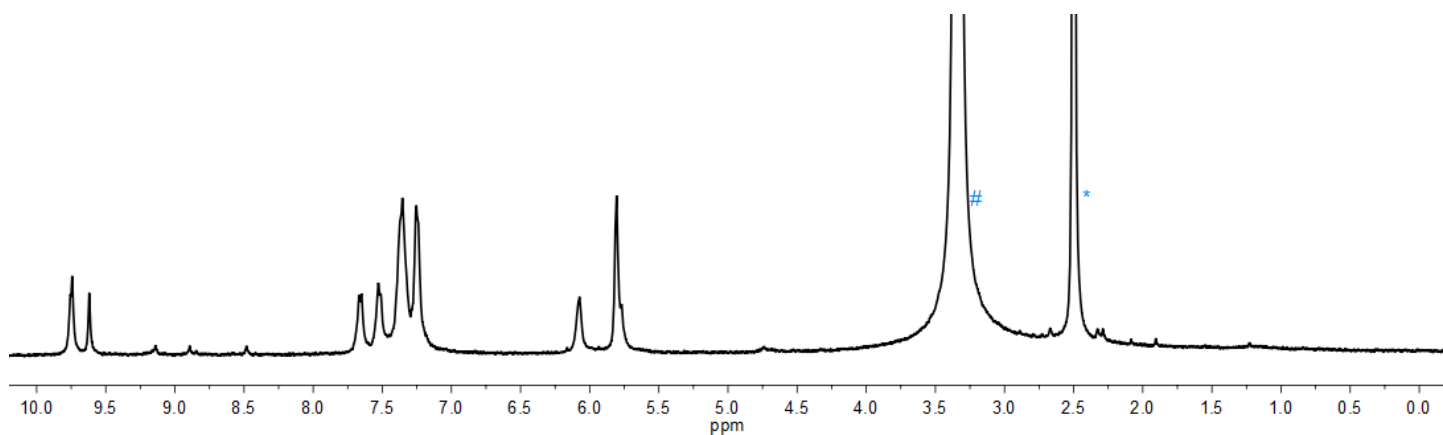


**Figure S26.**  $^1\text{H}$  NMR spectrum of  $4^1\text{-(BF}_4)_4$ , peak labelled \* results from incompletely deuterated NMR solvent and has been truncated, peak labelled # results from water and has been truncated ( $\text{d}_6\text{-DMSO}$ , 400 MHz, 298 K).

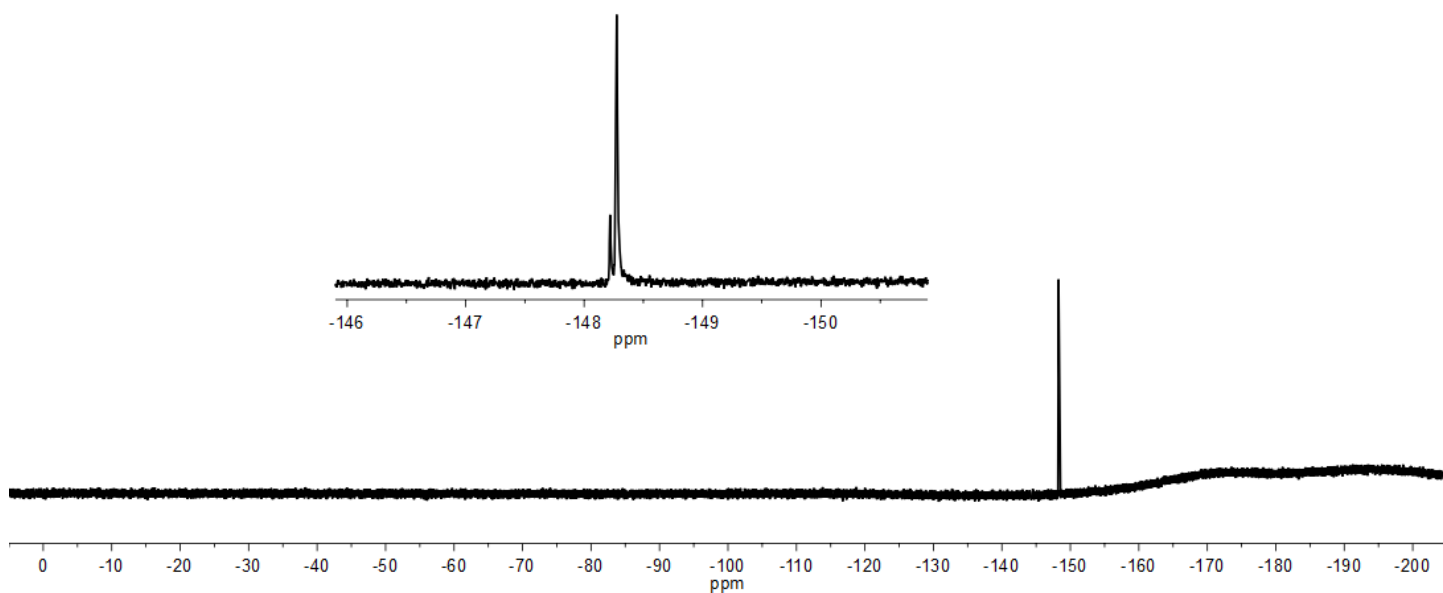


**Figure S27.**  $^{19}\text{F}$  NMR spectrum of  $4^1\text{-(BF}_4)_4$  ( $\text{d}_6\text{-DMSO}$ , 376 MHz, 298 K).

## Spectra for 6<sup>H</sup>-Cl:

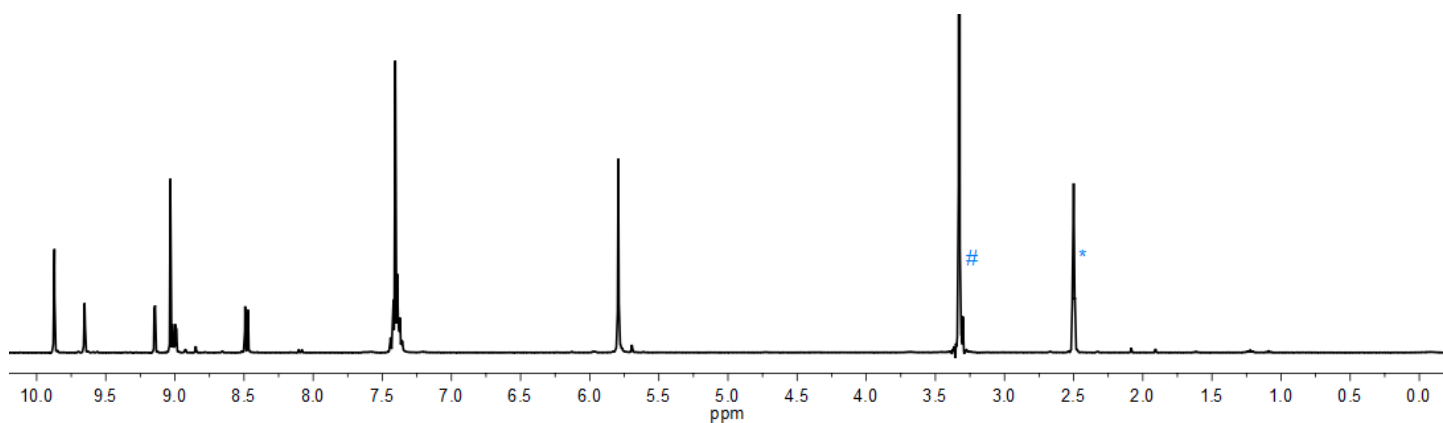


**Figure S28.** <sup>1</sup>H NMR spectrum of 6<sup>H</sup>-Cl, peak labelled \* results from incompletely deuterated NMR solvent, peak labelled # results from water and has been truncated (d<sub>6</sub>-DMSO, 400 MHz, 298 K).

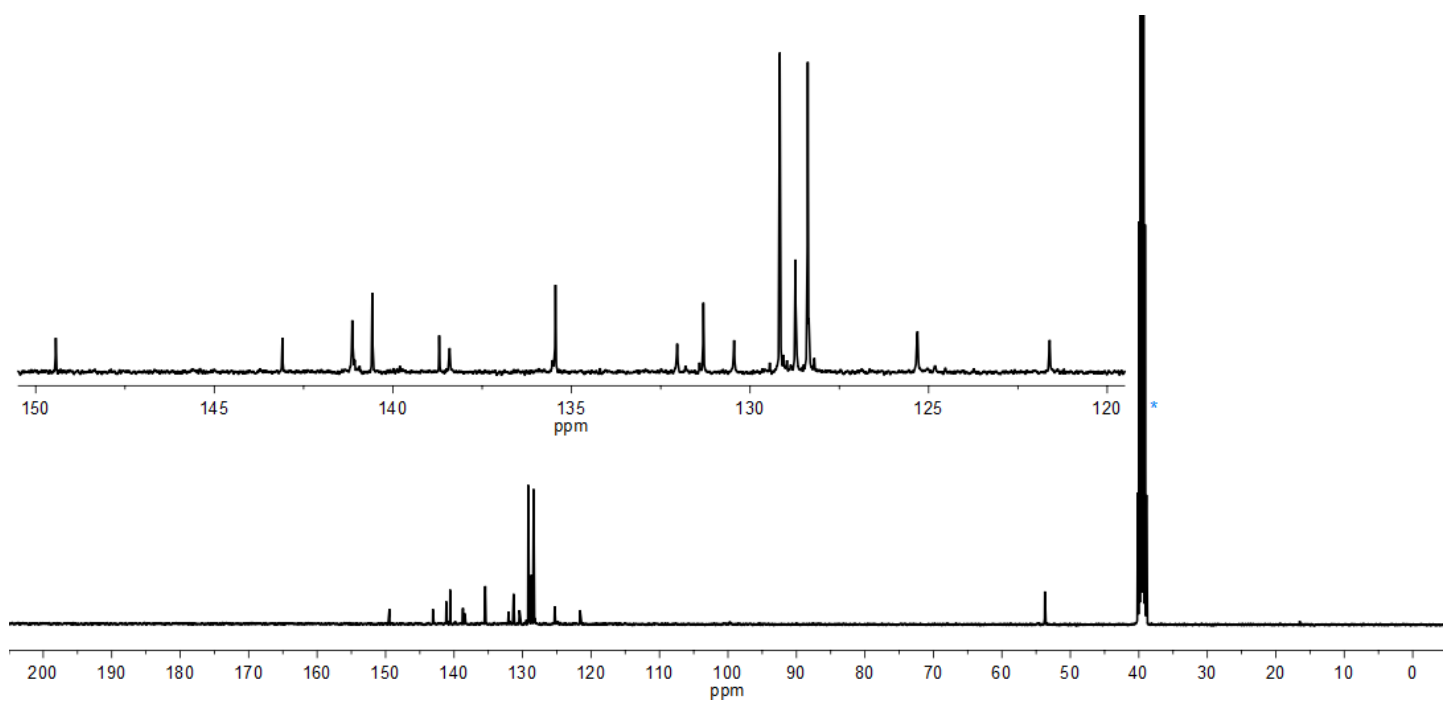


**Figure S29.** <sup>13</sup>C NMR spectrum of 6<sup>H</sup>-Cl, peak labelled \* results from incompletely deuterated NMR solvent and has been truncated (d<sub>6</sub>-DMSO, 101 MHz, 298 K).

## Spectra for 6<sup>1</sup>-Cl:

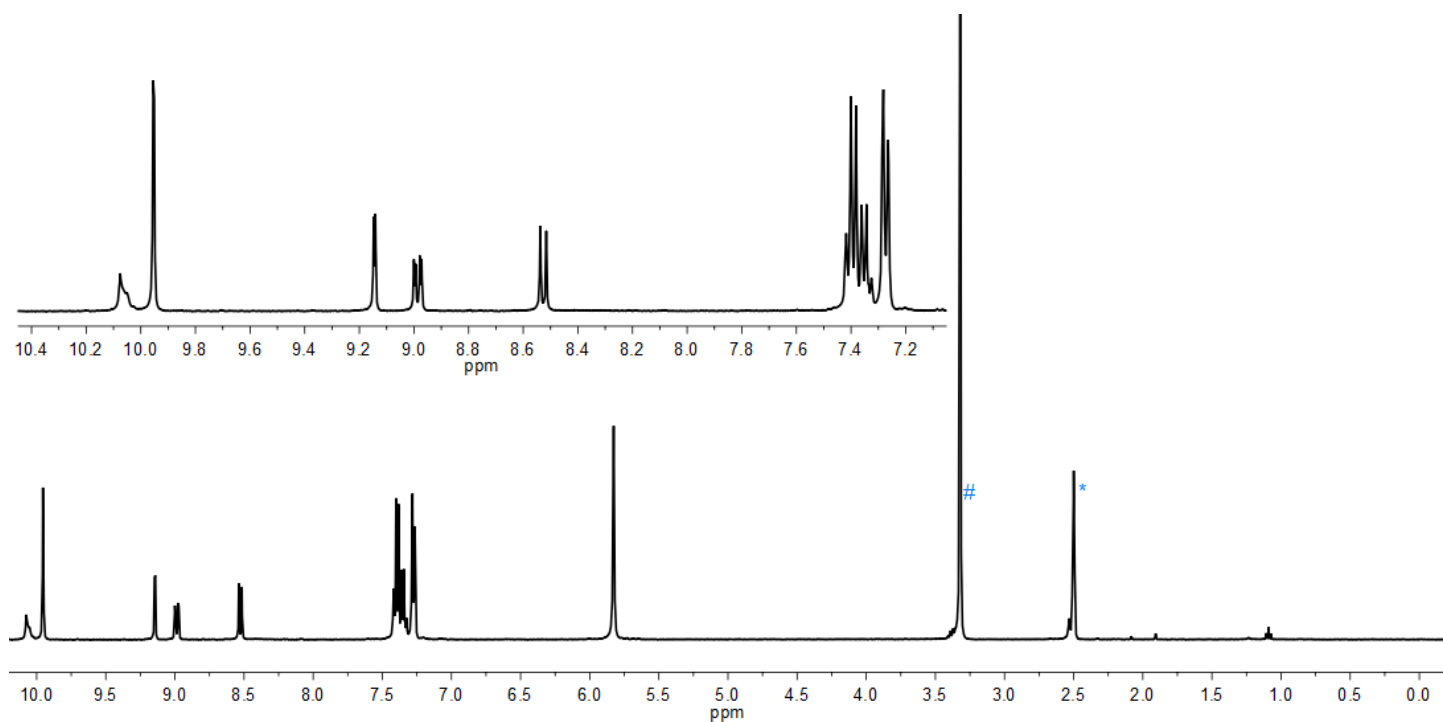


**Figure S30.** <sup>1</sup>H NMR spectrum of 6<sup>1</sup>-Cl, peak labelled \* results from incompletely deuterated NMR solvent, peak labelled # results from water and has been truncated (d<sub>6</sub>-DMSO, 400 MHz, 298 K).

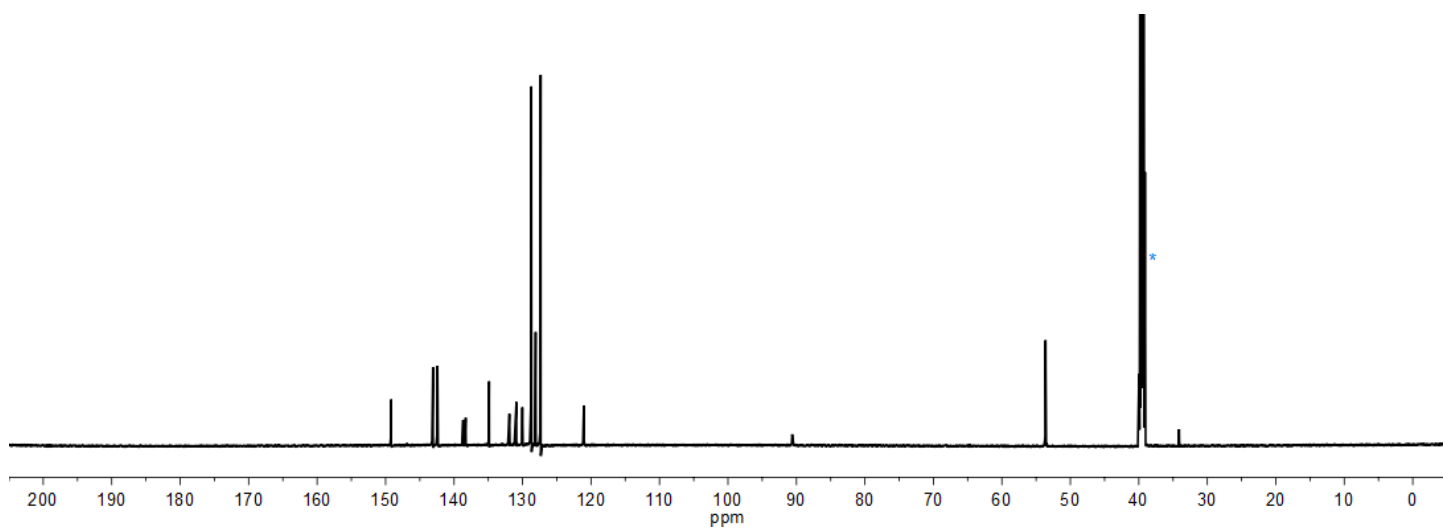


**Figure S31.** <sup>13</sup>C NMR spectrum of 6<sup>1</sup>-Cl, peak labelled \* results from incompletely deuterated NMR solvent and has been truncated (d<sub>6</sub>-DMSO, 151 MHz, 298 K).

Spectra for  $7^{\text{H}}\text{-Cl}_2$ :

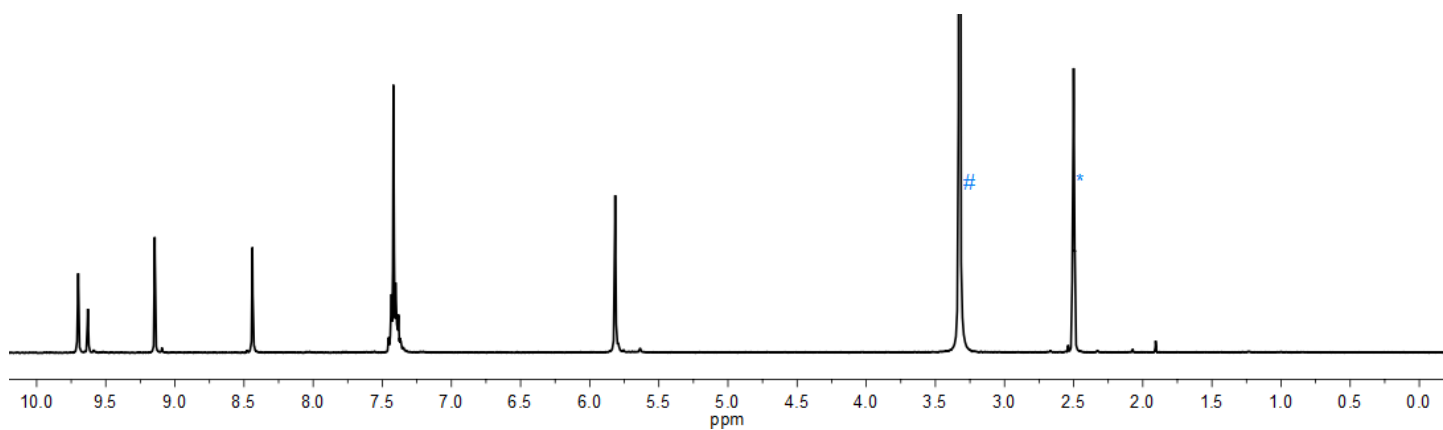


**Figure S32.**  $^1\text{H}$  NMR spectrum of  $7^{\text{H}}\text{-Cl}_2$ , peak labelled \* results from incompletely deuterated NMR solvent, peak labelled # results from water and has been truncated ( $\text{d}_6\text{-DMSO}$ , 400 MHz, 298 K).

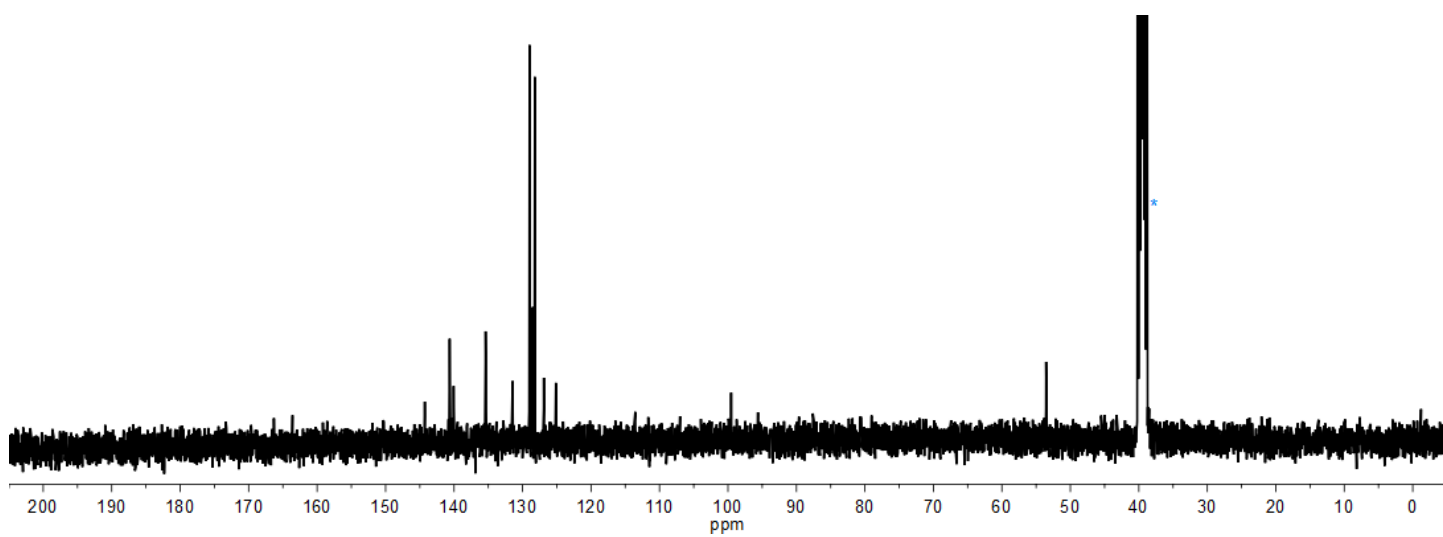


**Figure S33.**  $^{13}\text{C}$  NMR spectrum of  $7^{\text{H}}\text{-Cl}_2$ , peak labelled \* results from incompletely deuterated NMR solvent and has been truncated ( $\text{d}_6\text{-DMSO}$ , 101 MHz, 298 K).

Spectra for  $7^{\text{H}}\cdot(\text{PF}_6)_2$ :

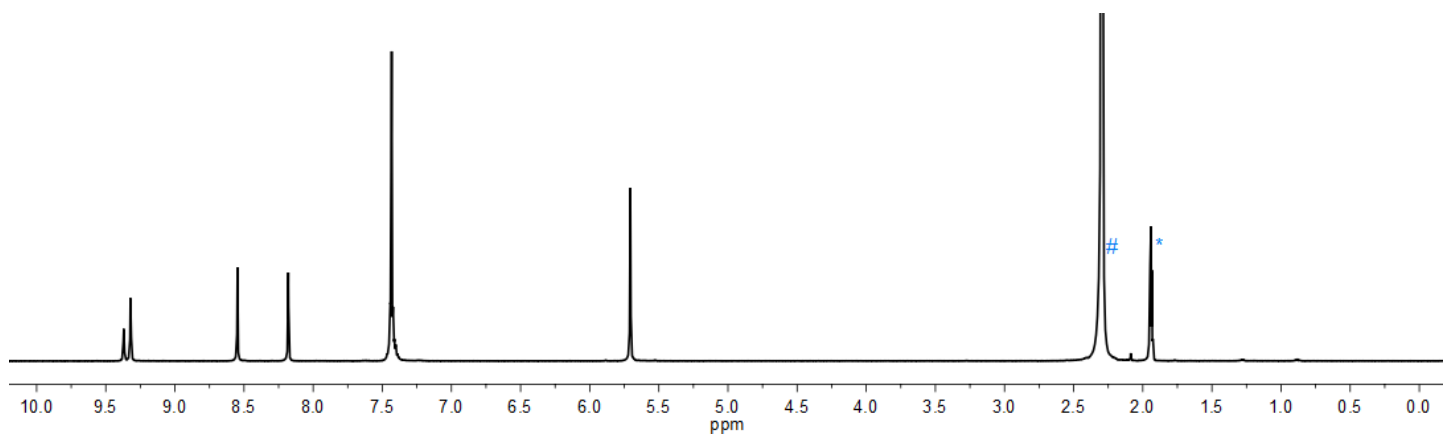


**Figure S34.**  $^1\text{H}$  NMR spectrum of  $7^{\text{H}}\cdot(\text{PF}_6)_2$ , peak labelled \* results from incompletely deuterated NMR solvent, peak labelled # results from water and has been truncated ( $\text{CD}_3\text{CN}$ , 400 MHz, 298 K).

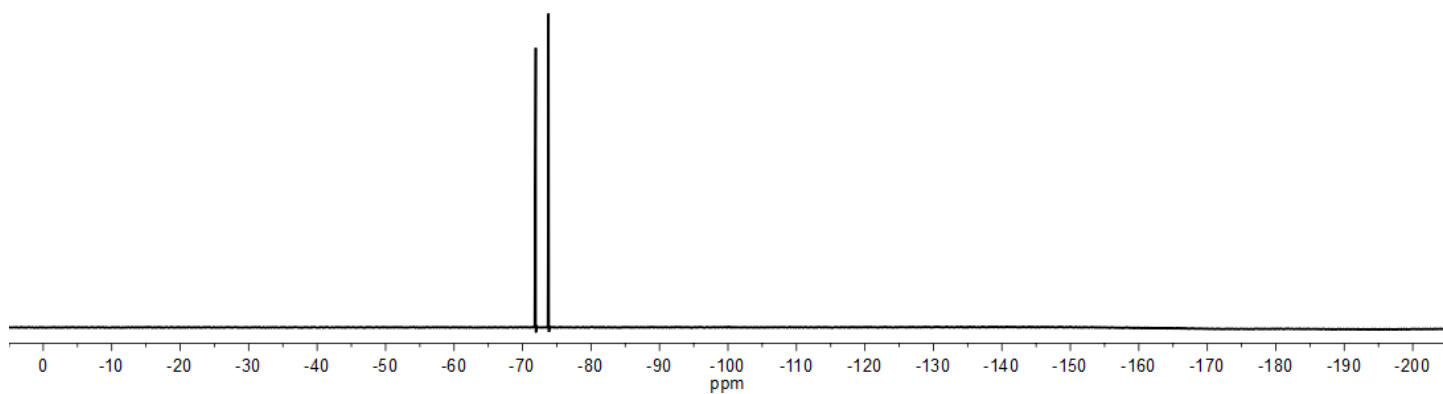


**Figure S35.**  $^{19}\text{F}$  NMR spectrum of  $7^{\text{H}}\cdot(\text{PF}_6)_2$  ( $\text{CD}_3\text{CN}$ , 376 MHz, 298 K).

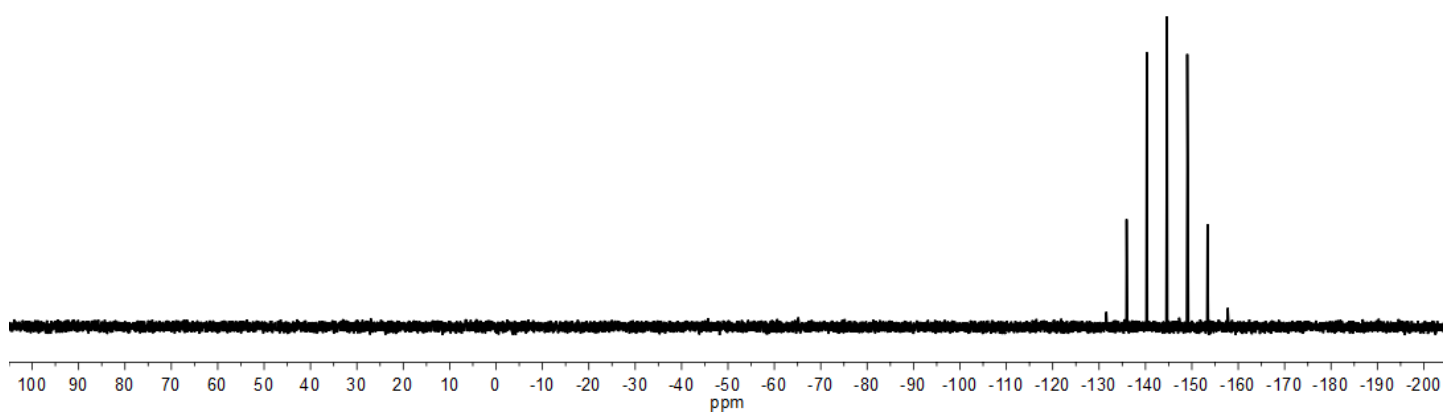


**Figure S36.**  $^{31}\text{P}$  NMR spectrum of  $7^{\text{H}}\cdot(\text{PF}_6)_2$  ( $\text{CD}_3\text{CN}$ , 162 MHz, 298 K).

## Spectra for $7^1\text{-Cl}_2$ :

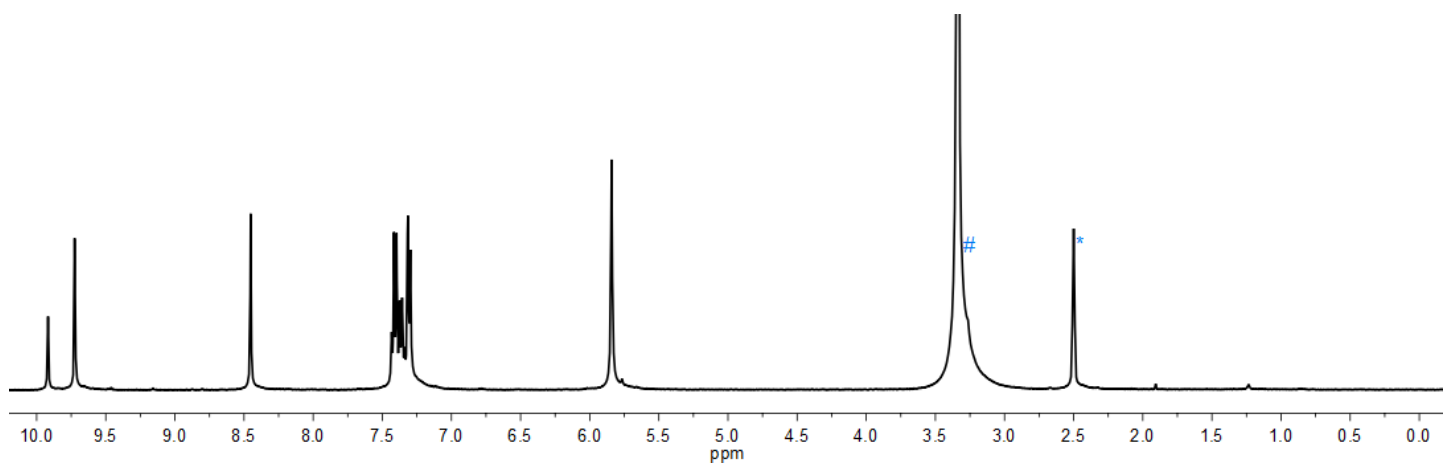


**Figure S37.**  $^1\text{H}$  NMR spectrum of  $7^1\text{-Cl}_2$ , peak labelled \* results from incompletely deuterated NMR solvent, peak labelled # results from water and has been truncated ( $d_6$ -DMSO, 400 MHz, 298 K).

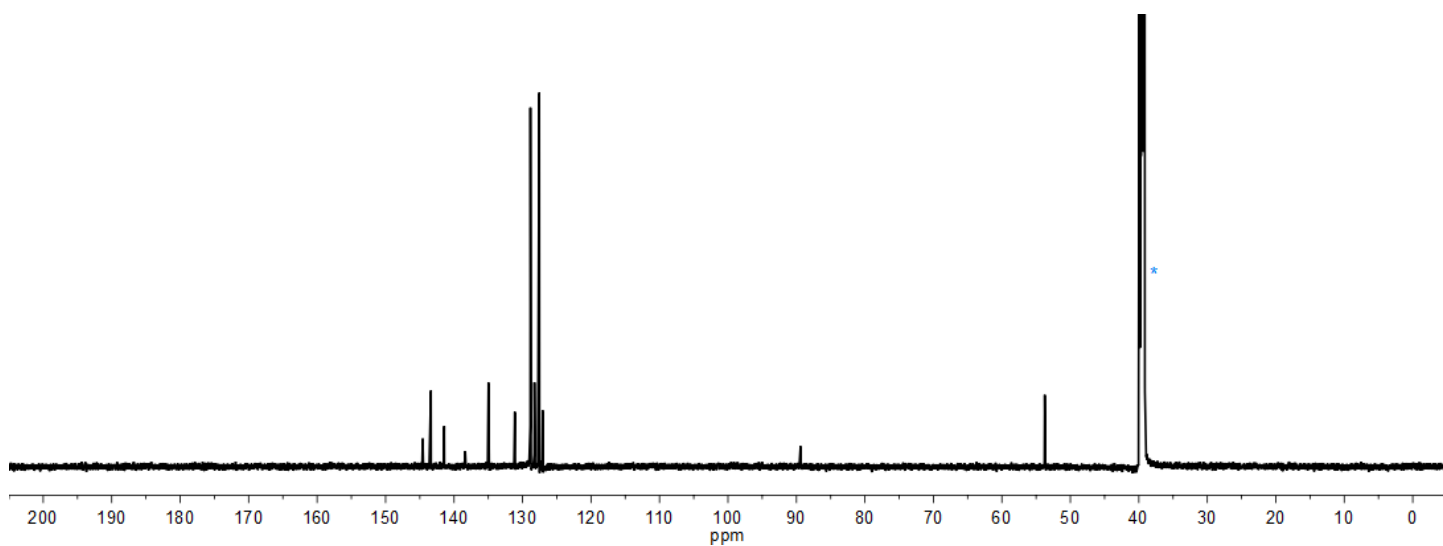


**Figure S38.**  $^{13}\text{C}$  NMR spectrum of  $7^1\text{-Cl}_2$ , peak labelled \* results from incompletely deuterated NMR solvent and has been truncated ( $d_6$ -DMSO, 176 MHz, 298 K).

### Spectra for $7^1\text{-(BF}_4)_2$ :

Note: due to the low yields of previous steps, this compound was only prepared on a very small scale (2 mg), and hence spectra are of relatively low quality.

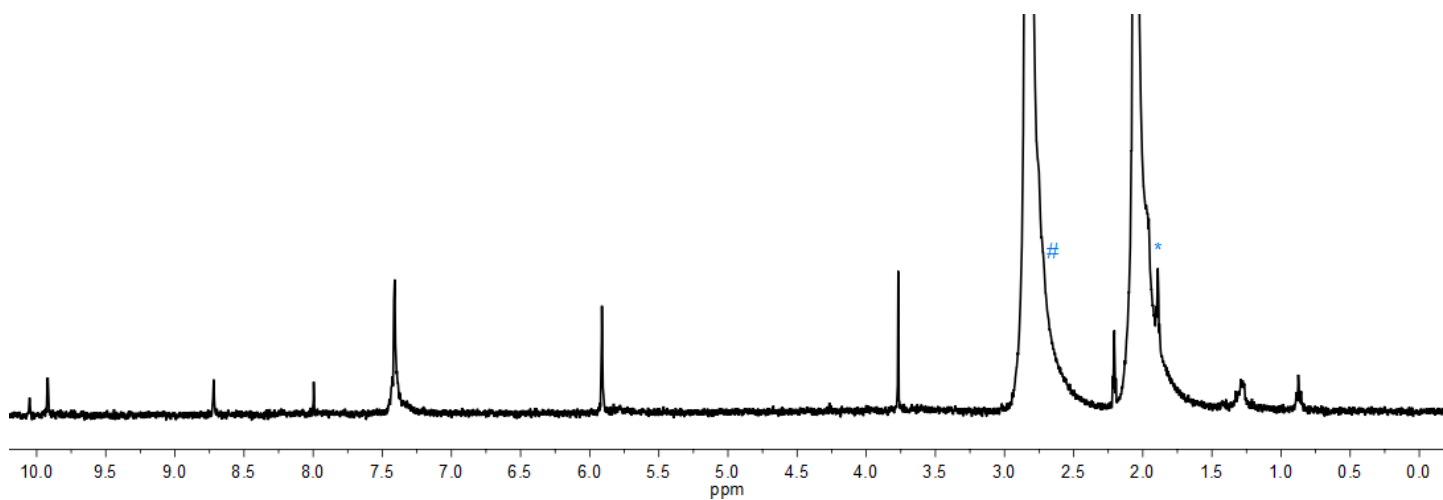


**Figure S39.**  $^1\text{H}$  NMR spectrum of  $7^1\text{-(BF}_4)_2$ , peak labelled \* results from incompletely deuterated NMR solvent and has been truncated, peak labelled # results from water and has been truncated ( $\text{d}_6\text{-DMSO}$ , 400 MHz, 298 K).

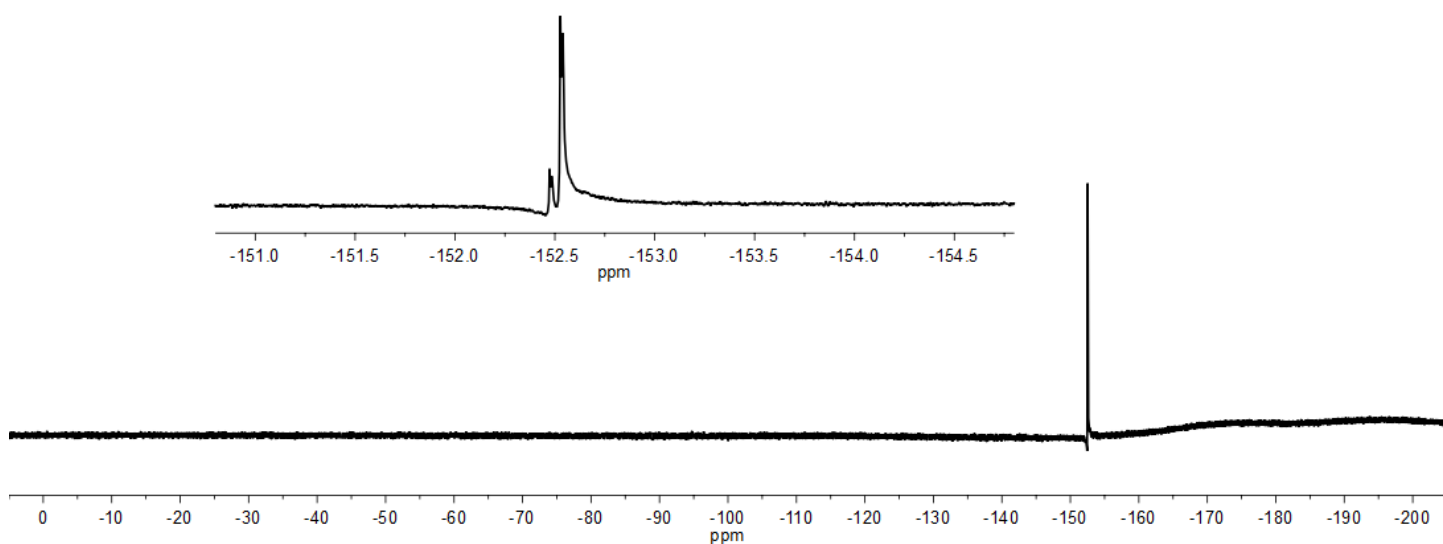


**Figure S40.**  $^{19}\text{F}$  NMR spectrum of  $7^1\text{-(BF}_4)_2$  ( $\text{d}_6\text{-DMSO}$ , 376 MHz, 298 K).

## Spectra for $8^{\text{H}}\text{-Cl}_4$

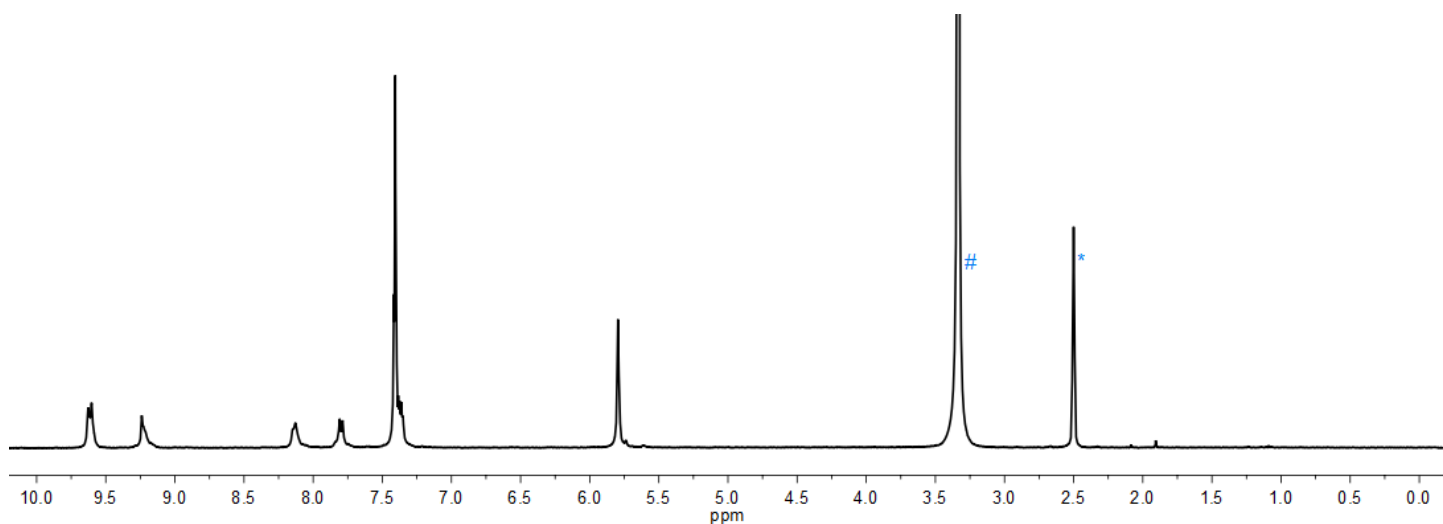


**Figure S41.**  $^1\text{H}$  NMR spectrum of  $8^{\text{H}}\text{-Cl}_4$ , peak labelled \* results from incompletely deuterated NMR solvent, peak labelled # results from water and has been truncated ( $\text{d}_6\text{-DMSO}$ , 400 MHz, 298 K).

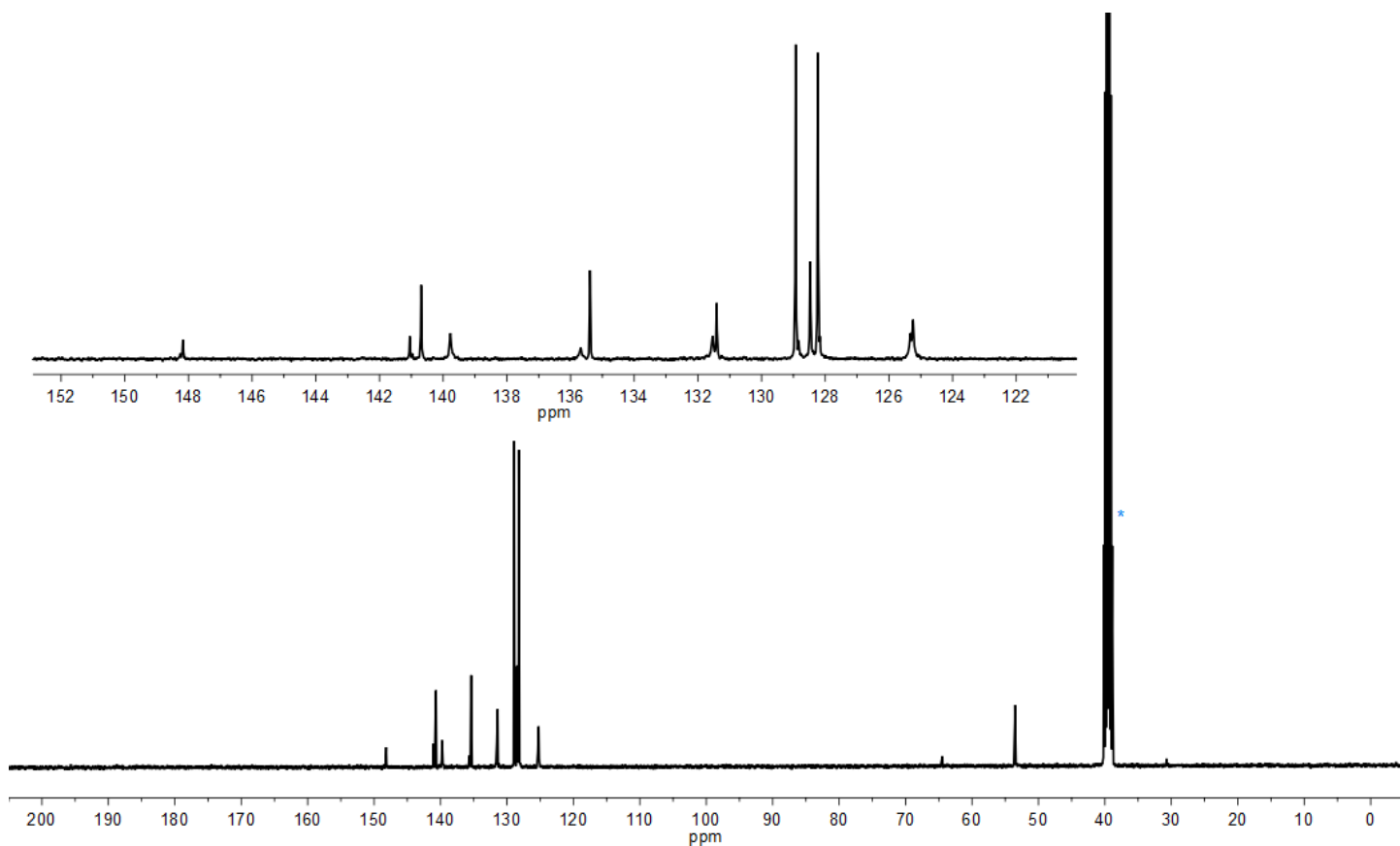


**Figure S42.**  $^{13}\text{C}$  NMR spectrum of  $8^{\text{H}}\text{-Cl}_4$ , peak labelled \* results from incompletely deuterated NMR solvent and has been truncated ( $\text{d}_6\text{-DMSO}$ , 101 MHz, 298 K).

Spectra for  $8^{\text{H}}\cdot(\text{PF}_6)_4$ :

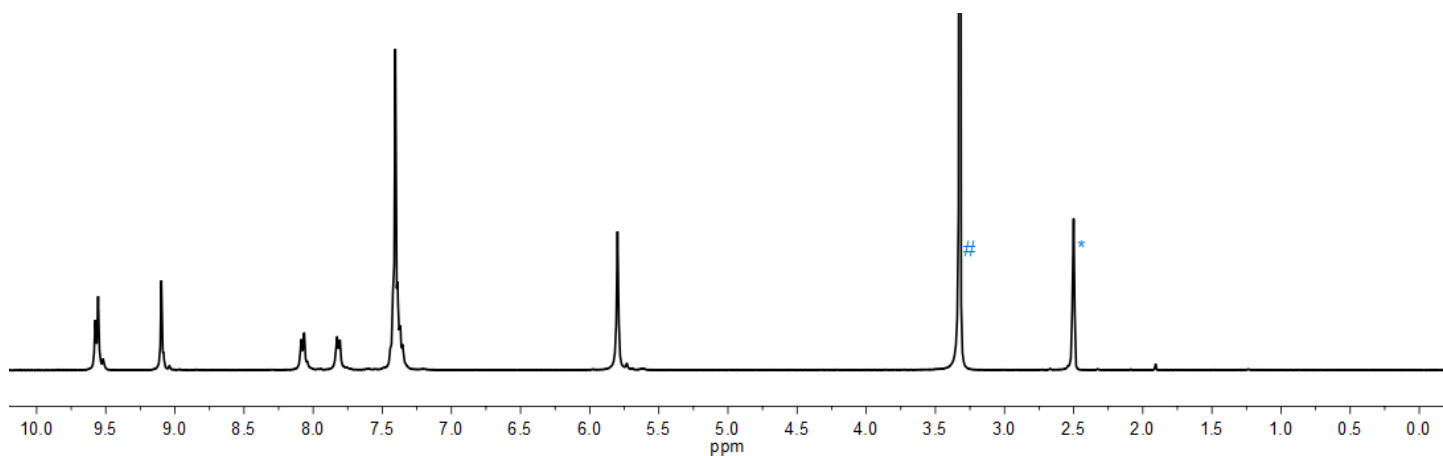


**Figure S43.**  $^1\text{H}$  NMR spectrum of  $8^{\text{H}}\cdot(\text{PF}_6)_4$ , peak labelled \* results from incompletely deuterated NMR solvent, peak labelled # results from water and has been truncated ( $\text{d}_6$ -DMSO, 400 MHz, 298 K).

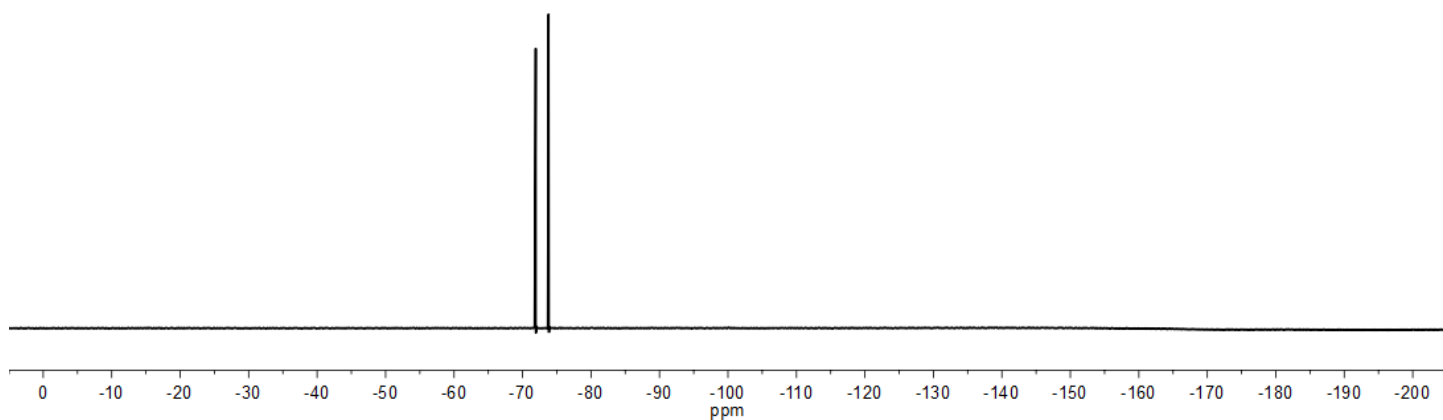


**Figure S44.**  $^{19}\text{F}$  NMR spectrum of  $8^{\text{H}}\cdot(\text{PF}_6)_4$  ( $\text{d}_6$ -DMSO, 376 MHz, 298 K).

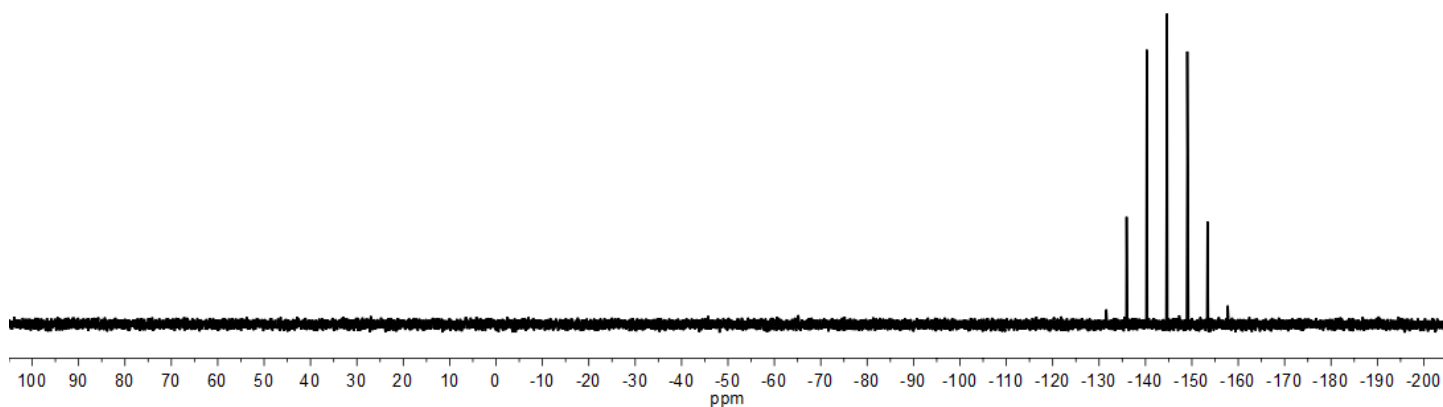


**Figure S45.**  $^{31}\text{P}$  NMR spectrum of  $8^{\text{H}}\cdot(\text{PF}_6)_4$  ( $\text{d}_6$ -DMSO, 162 MHz, 298 K).

## Optimised synthesis of 3,5-diethynylpyridine

This compound has been previously reported using a similar methodology,<sup>S2</sup> but we have found the procedure below to be optimal for our uses.

### 3,5-Bis(trimethylsilylethynyl)pyridine

A solution of 3,5-dibromopyridine (1.42 g, 6.00 mmol), Pd<sub>2</sub>dba<sub>3</sub> (0.092 g, 0.10 mmol), CuI (0.058 g, 0.30 mmol) and PPh<sub>3</sub> (0.262 g, 1.00 mmol) in NEt<sub>3</sub> (30 mL) was deoxygenated with bubbling N<sub>2</sub>. TMS-acetylene (2.12 mL, 15.0 mmol) was added and the reaction heated to 75 °C under an N<sub>2</sub> atmosphere for 18 hours. The resulting dark brown mixture was cooled to room temperature and filtered through a bed of celite, with the celite washed thoroughly with diethyl ether (7 × 25 mL). The resulting orange filtrate was taken to dryness under reduced pressure, and purified by column chromatography (dry-loaded, eluent: 5% ethyl acetate in pet. spirits) to give 3,5-bis(trimethylsilylethynyl)pyridine as orange crystals. Yield: 1.32 g (4.86 mmol, 81%). NMR data were consistent with those previously reported.<sup>S2</sup>

*We have found that filtering through celite is important to effectively remove inorganic impurities.*

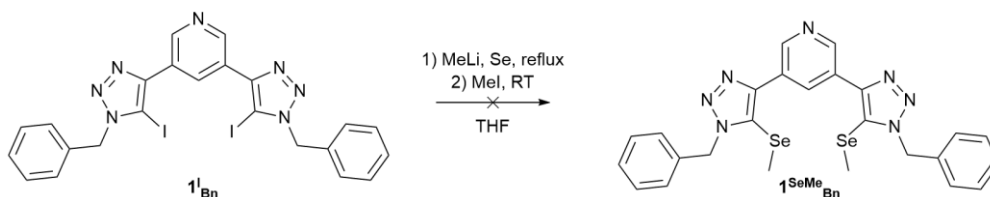
### 3,5-Diethynylpyridine

KOH (0.82 g, 15 mmol) in water (8 mL) was added to a solution of 3,5-bis(trimethylsilylethynyl)pyridine (1.32 g, 4.86 mmol, all of the previous reaction) in methanol (30 mL). This was stirred at room temperature for 30 minutes, then diluted with further water (40 mL) and extracted into pentane (5 × 100 mL). The organic layers were concentrated under slightly reduced pressure to obtain 3,5-diethynylpyridine as beige crystals. Yield: 0.610 g (4.80 mmol, 99%). NMR data were consistent with those previously reported.<sup>S2</sup>

*We found that far better yields were obtained by purifying the TMS-protected alkyne than by reacting on the crude TMS-protected product and purifying diethynylpyridine, as previously reported.<sup>S2</sup> Diethynylpyridine is prone to sublimation and it was found that it was best to remove pentane on a rotary evaporator using a mild vacuum (800–850 mbar) at modest temperatures (≤ 40 °C) to avoid the product subliming. If the reaction mixture was not diluted with further water prior to the pentane extraction step, then dramatically reduced yields were obtained.*

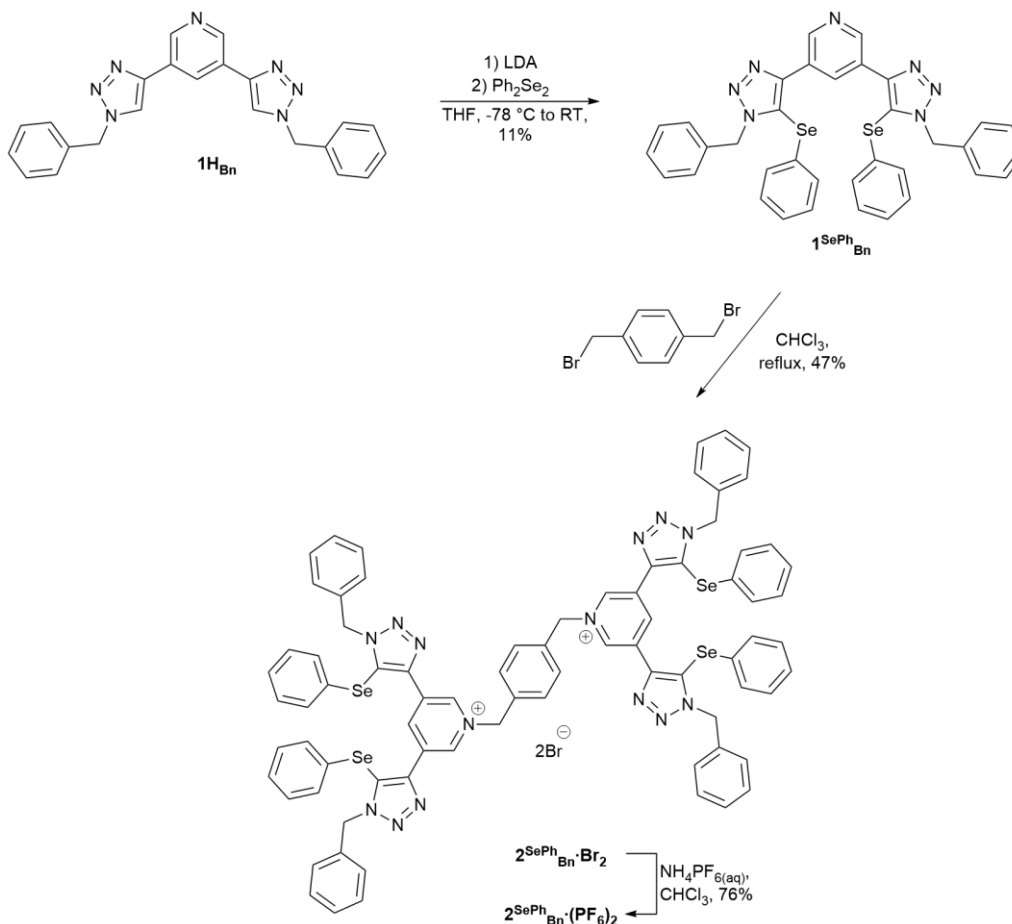
## Syntheses of selenium containing receptors

We initially tried to prepare the selenium **btp** derivative  $1^{\text{SeMe}}_{\text{Bn}}$  incorporating methyl-selenium groups at the 5-position of the triazole rings, using a procedure reported for a closely related compound (Scheme S1).<sup>S3</sup> However, we were unable to isolate clean  $1^{\text{SeMe}}_{\text{Bn}}$  using this procedure.



**Scheme S1.** Attempted synthesis of  $1^{\text{SeMe}}_{\text{Bn}}$ .

We were instead able to prepare  $1^{\text{SePh}}_{\text{Bn}}$ , which incorporates phenyl-selenium groups following a literature procedure for a related molecule,<sup>S4</sup> albeit in low yield (Scheme S2). Reaction of  $1^{\text{SePh}}_{\text{Bn}}$  with 1,4-bis(bromomethyl)benzene gave the ditopic receptor  $2^{\text{SePh}}_{\text{Bn}} \cdot \text{Br}_2$ , and subsequent anion exchange gave  $2^{\text{SePh}}_{\text{Bn}} \cdot (\text{PF}_6)_2$ . For solubility reasons, it was necessary to conduct the alkylation reaction to give  $2^{\text{SePh}}_{\text{Bn}} \cdot \text{Br}_2$  in chloroform, rather than in acetonitrile, which was used in the reactions to prepare  $2^{\text{H}}_{\text{hex}} \cdot \text{Br}_2$ ,  $2^{\text{H}}_{\text{Bn}} \cdot \text{Br}_2$  and  $2^{\text{I}}_{\text{Bn}} \cdot \text{Br}_2$ .



**Scheme S2.** Synthesis of  $1^{\text{SePh}}_{\text{Bn}}$  and  $2^{\text{SePh}}_{\text{Bn}}^{2+}$ .

Despite several attempts we were unable to obtain any crystals from  $2^{\text{SePh}}_{\text{Bn}}^{2+}$ . We were also unable to prepare  $4^{\text{SePh}}_{\text{Bn}} \cdot \text{Br}_4$  by heating  $1^{\text{SePh}}_{\text{Bn}}$  and **3** in boiling chloroform or toluene for extended periods. While  $^1\text{H}$  NMR spectroscopy suggested some reaction had occurred, it was not possible to isolate any product from the large amounts of unreacted starting materials.

### Synthesis of $1^{\text{SePh}}_{\text{Bn}}$

In a dry Schlenk flask,  $1^{\text{H}}_{\text{Bn}}$  (0.500 g, 1.26 mmol, 1.0 equiv.) was dissolved in dry THF (40 mL) under a nitrogen atmosphere. The solution was cooled to  $-78\text{ }^{\circ}\text{C}$  and a solution of LDA in THF/hexanes (1.0 M, 2.5 mL, 2.5 mmol, 2.0 equiv.) was added slowly causing the solution to change colour from pale yellow to blood red. It was stirred at  $-78\text{ }^{\circ}\text{C}$  for 3 hours, and then a solution of diphenyl diselenide (0.990 g, 3.17 mmol, 2.5 equiv.) in dry THF (30 mL) was added causing a colour change to brown. The reaction was stirred at this temperature for another 2 hours and then left to warm to room temperature overnight. The crude mixture was then concentrated under reduced pressure to give a brown oily solid. This was purified by column chromatography (eluting with 6:4 ethyl acetate: pet. spirits then 3:7 acetonitrile:dichloromethane) to give  $1^{\text{SePh}}_{\text{Bn}}$  as a colourless oil that solidified on standing. Yield: 0.100 g (0.142 mmol, 11%).

*Note: all glassware from this reaction was left to sit in a bleach solution overnight to remove any odour.*

$^1\text{H}$  NMR ( $\text{CDCl}_3$ ): 9.23 (d,  $J = 2.1$  Hz, 2H), 9.03 (t,  $J = 2.1$  Hz, 1H), 7.20–7.26 (m, 10H), 7.10 (d,  $J = 7.1$  Hz, 2H), 7.05 (dd,  $J = 7.2, 7.1$  Hz, 4H), 6.93 (d,  $J = 7.2$  Hz, 4H), 5.66 (s, 4H) ppm.  $^{13}\text{C}$  NMR ( $\text{CDCl}_3$ ): 148.7, 148.3, 134.7, 133.1, 129.93, 129.90, 129.1, 128.9, 128.5, 128.1, 127.7, 126.5, 119.4, 53.4 ppm.  $^{77}\text{Se}$  NMR ( $\text{CDCl}_3$ ): 228.1 (s) ppm. HRESI-MS (pos): 706.0742, calc. for  $[\text{C}_{35}\text{H}_{27}\text{N}_7^{80}\text{Se}_2\text{H}]^+ = 706.0737$  Da.

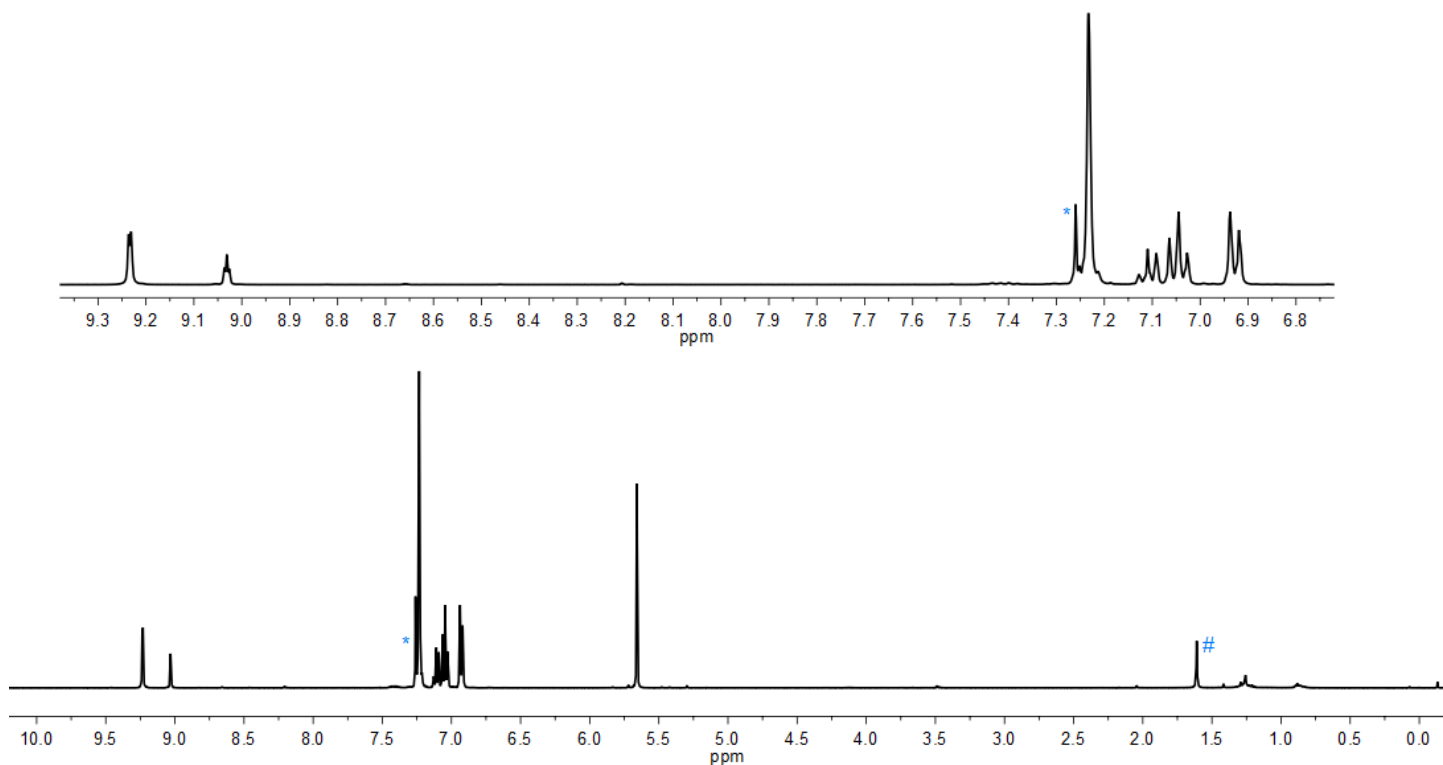


**Figure S46.**  $^1\text{H}$  NMR spectrum of  $1^{\text{SePh}}_{\text{Bn}}$ , peak labelled \* results from incompletely deuterated NMR solvent, peak labelled # results from water ( $\text{CDCl}_3$ , 400 MHz, 298 K).

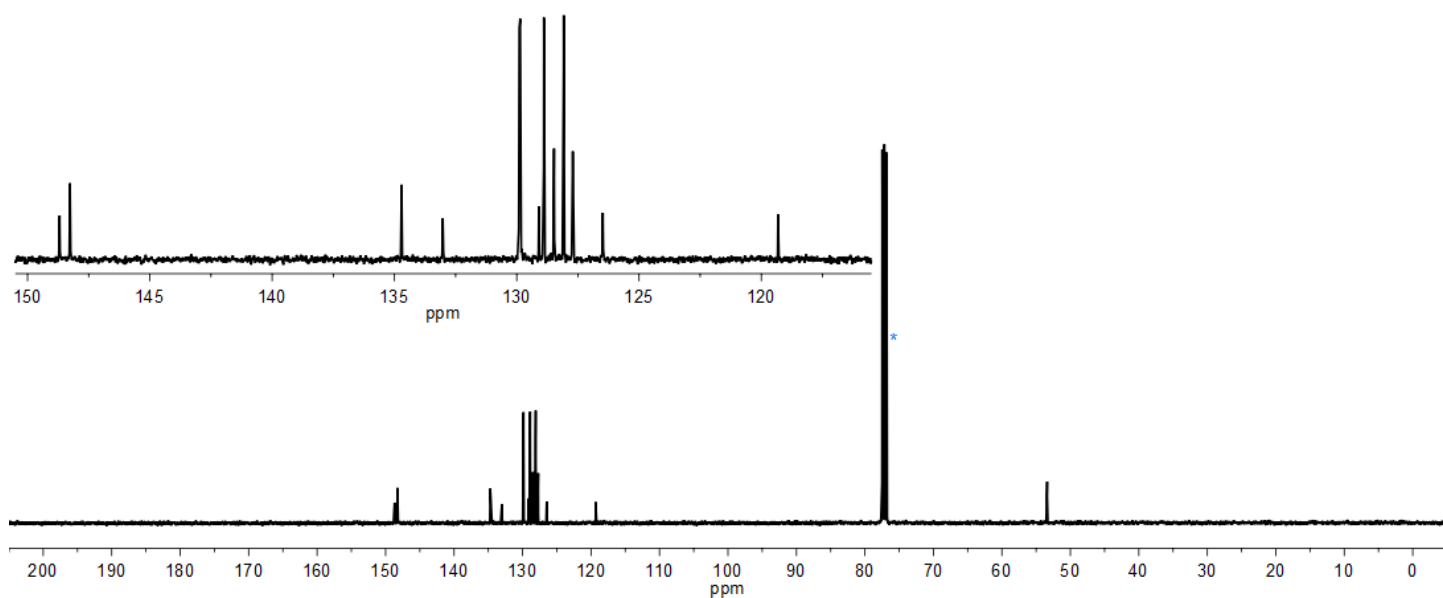


**Figure S47.**  $^{13}\text{C}$  NMR spectrum of  $1^{\text{SePh}}_{\text{Bn}}$ , peak labelled \* results from incompletely deuterated NMR solvent ( $\text{CDCl}_3$ , 101 MHz, 298 K).

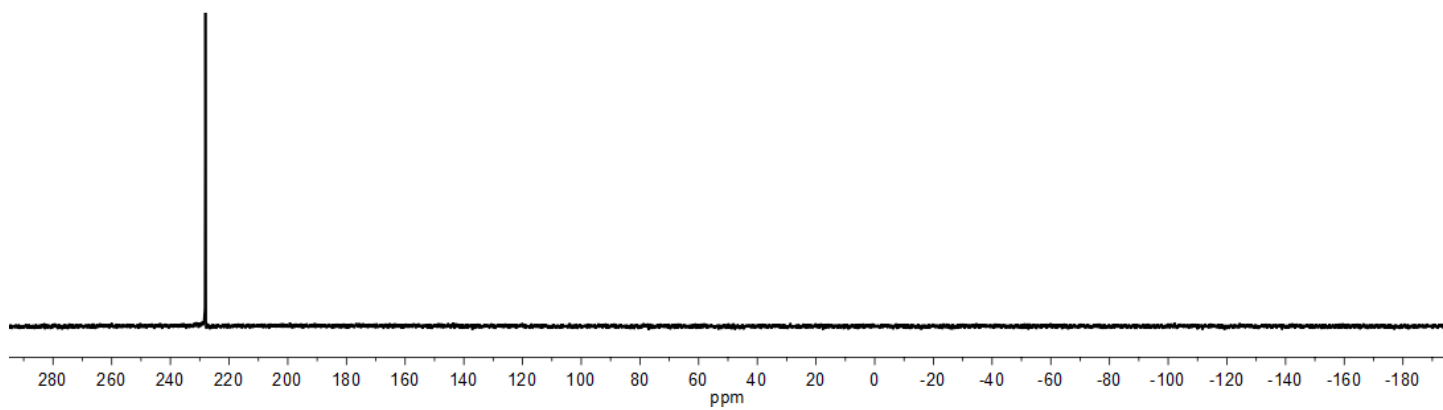


**Figure S48.**  $^{77}\text{Se}$  NMR spectrum of  $1^{\text{SePh}}_{\text{Bn}}$  ( $\text{CDCl}_3$ , 134 MHz, 298 K).

### Synthesis of $2^{\text{SePh}}_{\text{Bn}}\cdot\text{Br}_2$

$1^{\text{SePh}}_{\text{Bn}}$  (0.062 g, 0.087 mmol, 2.0 equiv.) and 1,4-bis(bromomethyl)benzene (0.012 g, 0.043 mmol, 1.0 equiv.) were dissolved in chloroform (5 mL) and the pale yellow solution was heated to reflux under nitrogen for 5 days. It was then cooled to room temperature and concentrated under reduced pressure to give a yellow oil. Column chromatography (9:1 dichloromethane:methanol) gave  $2^{\text{SePh}}_{\text{Bn}}\cdot\text{Br}_2$  as a yellow glassy solid. Yield: 0.034 g (0.020 mmol, 47%).

$^1\text{H}$  NMR ( $\text{CDCl}_3$ ): 9.86 (s, 4H), 9.76 (s, 2H), 7.59 (s, 4H), 7.11–7.21 (m, 24H), 7.04 (dd,  $J = 7.6, 7.4$  Hz, 8H), 6.88 (d,  $J = 7.6$  Hz, 8H), 6.35 (s, 4H), 5.63 (s, 8H) ppm.  $^{13}\text{C}$  NMR ( $\text{CDCl}_3$ ): 143.7, 140.8, 138.9, 134.5, 133.9, 132.1, 131.0, 130.3, 130.2, 129.0, 128.7, 128.3, 128.2, 128.1, 122.5, 64.6, 53.4 ppm.  $^{77}\text{Se}$  NMR ( $\text{CDCl}_3$ ): 235.9 (s) ppm. HRESI-MS (pos): 757.0951, calc. for  $[\text{C}_{78}\text{H}_{62}\text{N}_{14}^{80}\text{Se}_4]^{2+} = 757.0971$  Da.

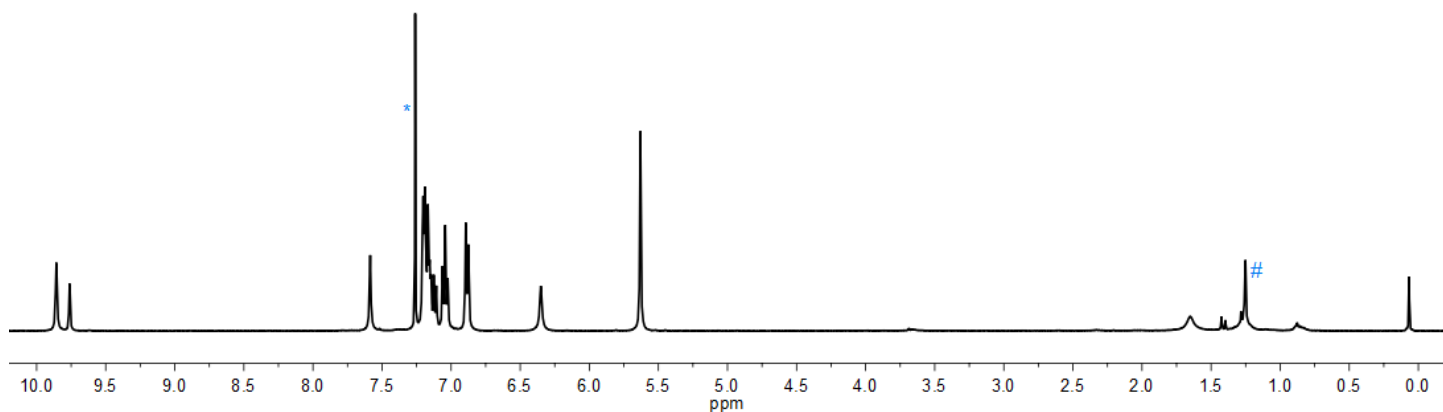


**Figure S49.**  $^1\text{H}$  NMR spectrum of  $2^{\text{SePh}}_{\text{Bn}}\cdot\text{Br}_2$ , peak labelled \* results from incompletely deuterated NMR solvent, peak labelled # results from water ( $\text{CDCl}_3$ , 400 MHz, 298 K).

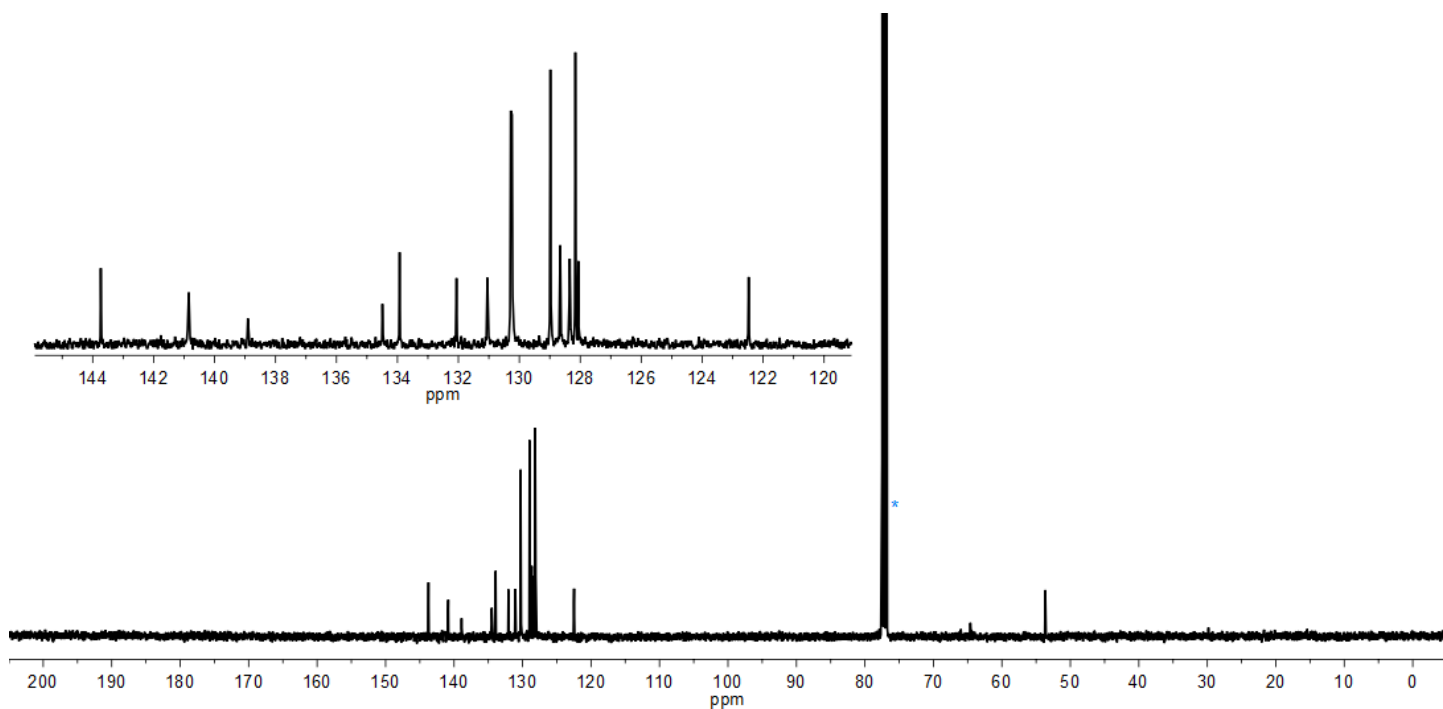


**Figure S50.**  $^{13}\text{C}$  NMR spectrum of  $2^{\text{SePh}}_{\text{Bn}}\cdot\text{Br}_2$ , peak labelled \* results from incompletely deuterated NMR solvent and has been truncated ( $\text{CDCl}_3$ , 101 MHz, 298 K).

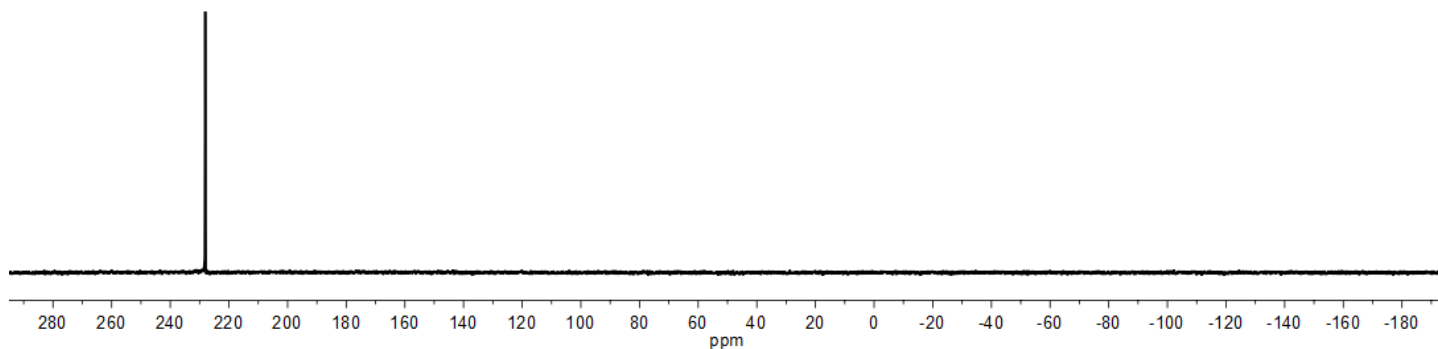


**Figure S51.**  $^{77}\text{Se}$  NMR spectrum of  $2^{\text{SePh}}_{\text{Bn}}\text{Br}_2$  ( $\text{CDCl}_3$ , 134 MHz, 298 K).

### Synthesis of $2^{\text{SePh}}_{\text{Bn}}(\text{PF}_6)_2$

A solution of  $2^{\text{SePh}}_{\text{Bn}}\text{Br}_2$  (0.027 g, 0.016 mmol) in chloroform (20 mL) was washed with  $\text{NH}_4\text{PF}_6(\text{aq})$  (0.1 M, 10  $\times$  10 mL). The organic layer was then washed with brine (10 mL), dried ( $\text{MgSO}_4$ ) and taken to dryness under reduced pressure to give  $2^{\text{SePh}}_{\text{Bn}}(\text{PF}_6)_2$  as a glassy pale yellow solid. Yield: 0.022 g (0.012 mmol, 76%).

$^1\text{H}$  NMR ( $\text{CDCl}_3$ ): 9.82 (s, 2H), 9.33 (s, 4H), 7.33 (s, 4H), 7.03–7.17 (m, 24H), 7.00 (dd,  $J = 7.6, 7.4$  Hz, 8H), 6.86 (d,  $J = 7.4$  Hz, 8H), 5.75 (s, 4H), 5.56 (s, 8H) ppm.  $^{19}\text{F}$  NMR ( $\text{CDCl}_3$ ):  $-72.1$  (d,  $J = 714$  Hz) ppm.  $^{31}\text{P}$  NMR ( $\text{CDCl}_3$ ):  $-144.5$  (hept.,  $J = 714$  Hz) ppm. ESI-MS (pos.): 1657.4, calc. for  $[(\text{C}_{78}\text{H}_{62}\text{N}_{14}\text{Se}_4)^{2+}(\text{PF}_6)^-]_2^+$  = 1657.2 Da.

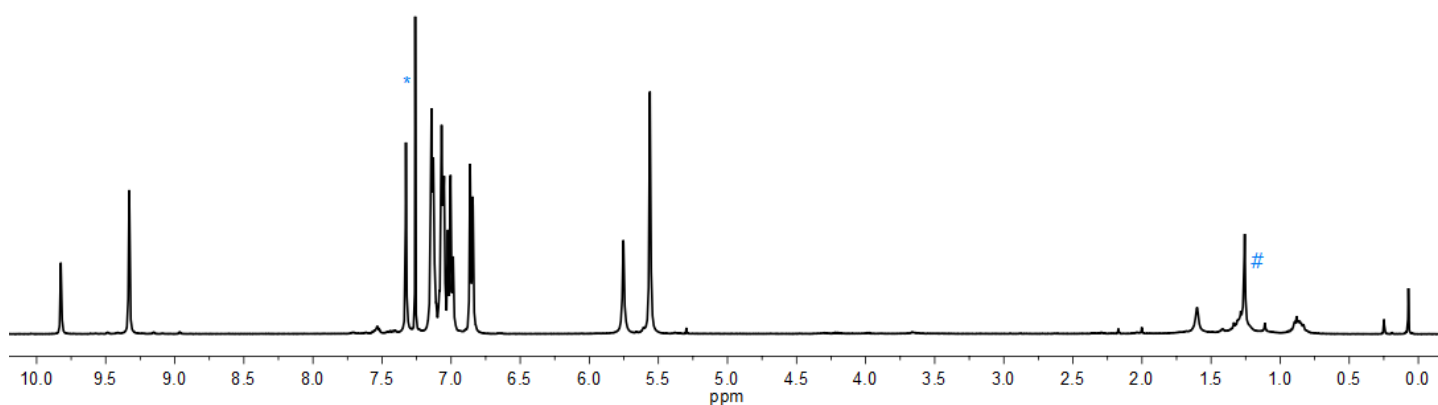


**Figure S52.**  $^1\text{H}$  NMR spectrum of  $2^{\text{SePh}}_{\text{Bn}}(\text{PF}_6)_2$ , peak labelled \* results from incompletely deuterated NMR solvent, peak labelled # results from water ( $\text{CDCl}_3$ , 400 MHz, 298 K).

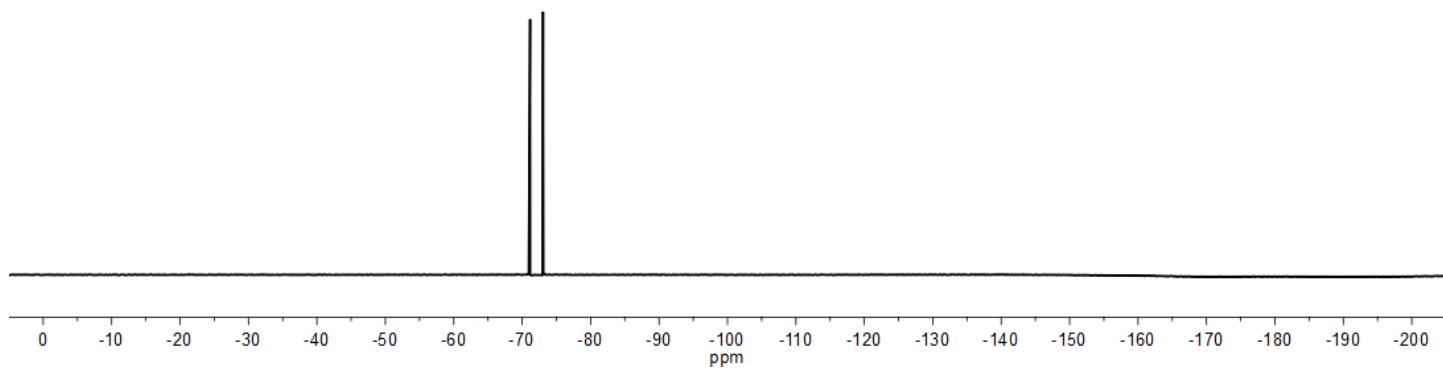


**Figure S53.**  $^{19}\text{F}$  NMR spectrum of  $2^{\text{SePh}}_{\text{Bn}}(\text{PF}_6)_2$  ( $\text{CDCl}_3$ , 376 MHz, 298 K).

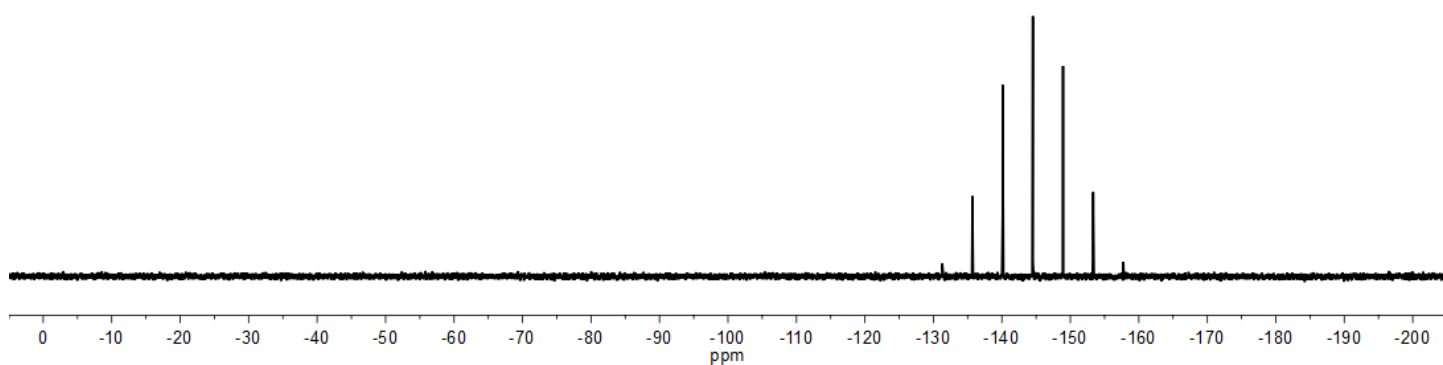


**Figure S54.**  $^{31}\text{P}$  NMR spectrum of  $2^{\text{SePh}}_{\text{Bn}}(\text{PF}_6)_2$  ( $\text{CDCl}_3$ , 161 MHz, 298 K).

# X-ray crystallography

## *Details of data collection and refinement*

### **Structures collected on home source diffractometer**

The structures of  $1^{\text{H}}_{\text{Bn}}$  and  $2^{\text{I}}_{\text{Bn}}(\text{HSO}_4)_2$  were collected on a dual-source Oxford Diffraction Supernova instrument at 150 K. Cu K $\alpha$  radiation was used for  $1^{\text{H}}_{\text{Bn}}$  and Mo K $\alpha$  radiation was used for  $2^{\text{I}}_{\text{Bn}}(\text{HSO}_4)_2$ . Raw frame data (including data reduction, interframe scaling, unit cell refinement and absorption corrections) were processed using CrysAlis Pro.<sup>S5</sup>

### **Structures collected at the Australian Synchrotron**

The structures of  $2^{\text{H}}_{\text{hex}}(\text{HSO}_4)_2$  and  $2^{\text{I}}_{\text{Bn}}(\text{HSO}_4)_2$  were collected using the MX1 beamline<sup>S6</sup> of the Australian Synchrotron, while structures of  $2^{\text{I}}_{\text{Bn}}\cdot\text{Cl}_2$ ,  $7^{\text{H}}\cdot\text{Cl}_2$  and  $8^{\text{H}}\cdot(\text{SO}_4)_2$  were collected using the MX2 beamline<sup>S7</sup> of the Australian Synchrotron. All synchrotron structures were collected at 100 K, and raw frame data were processed using XDS.<sup>S8</sup>

### **Structure refinements**

The structures  $1^{\text{H}}_{\text{Bn}}$ ,  $2^{\text{I}}_{\text{Bn}}(\text{HSO}_4)_2$ ,  $2^{\text{I}}_{\text{Bn}}(\text{HSO}_4)_{1.2}\cdot\text{Br}_{0.8}$  and  $7^{\text{H}}\cdot\text{Cl}_2$  were solved using SHELXT,<sup>S9</sup> and the structures of  $2^{\text{H}}_{\text{hex}}(\text{HSO}_4)_2$ ,  $2^{\text{I}}_{\text{Bn}}\cdot\text{Cl}_2$  and  $8^{\text{H}}\cdot(\text{SO}_4)_2$  were solved using SuperFlip.<sup>S10</sup> All structures were refined within the Crystals suite,<sup>S11</sup> except for the structure of  $7^{\text{H}}\cdot\text{Cl}_2$ , which was refined within OLEX2.<sup>S12</sup> Unless otherwise stated, all non-hydrogen atoms were refined with anisotropic displacement parameters. Details of individual refinements are provided in the following section, with thermal ellipsoid plots provided in Figures S55–S61.

Full crystallographic data in CIF format are have been deposited with the Cambridge Structural Database (CCDC Numbers: 2130560 – 2130566). Crystallographic data are summarised in Table S1.

## Details of individual refinements

### **1<sup>H</sup><sub>Bn</sub>**

The asymmetric unit contains two molecules of the compound, and there appears to be a water molecule sitting within the "cleft" of each of these. However, the ellipsoids for these water molecules were highly elongated and chemically unreasonable. Attempts to model these as disordered over two adjacent sites were unsuccessful, as were attempts to restrain the ellipsoid parameters using ISOR restraints (within OLEX2<sup>S12</sup>). Therefore PLATON-SQUEEZE<sup>S13</sup> was used to include the electron density in the refinement.

One of the phenyl rings of each molecule had enlarged ellipsoids and chemically unreasonable bond lengths, so restraints were added to C–C bond lengths, and thermal and vibrational ellipsoid parameters for these parts of the molecule. C–H hydrogen atoms were generally visible in the Fourier difference map, and were initially refined with restraints on bond lengths and angles, after which the positions were used as the basis for a riding model.<sup>S14</sup>

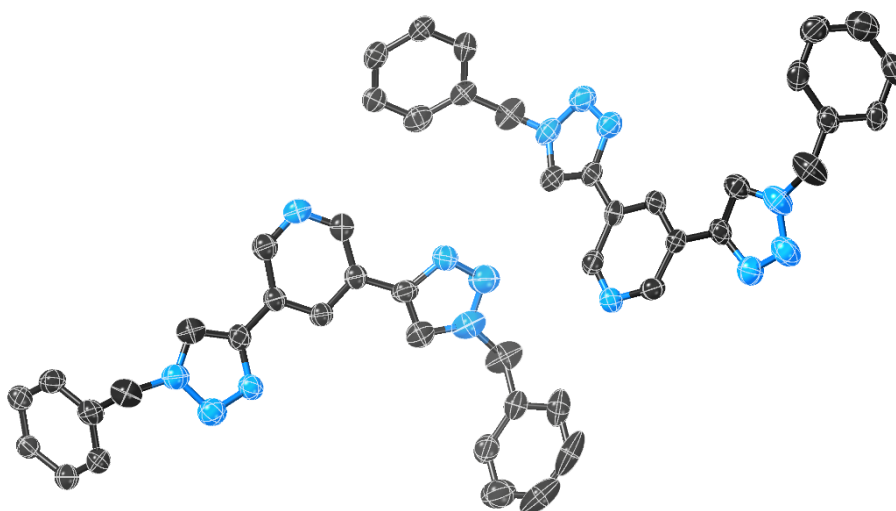


**Figure S55.** Thermal ellipsoid plot showing the asymmetric unit of **1<sup>H</sup><sub>Bn</sub>**. Ellipsoids are shown at 50% probability, hydrogen atoms are omitted for clarity. PLATON-SQUEEZE<sup>S13</sup> was used.

## $2^{\text{H}}_{\text{hex}} \cdot (\text{HSO}_4)_2$

Crystals were small and very weakly diffracting, and required the use of synchrotron radiation. Even using synchrotron radiation, diffraction was weak and it was not possible to observe diffraction beyond 1.0 Å. The hexyl chains of the molecule are very ill-defined. Each of the two crystallographically unique hexyl groups was modelled over two sites, with restraints added to C–C bond lengths and bond angles in order to achieve a chemically sensible refinement. Even with these restraints, it was necessary to model the carbon atoms of these hexyl chains isotropically in order to achieve a sensible refinement. A region of poorly-defined electron density, believed to arise from solvent molecules was present but could not be modelled. PLATON-SQUEEZE<sup>S13</sup> was used to include this electron density in the refinement.

Generally, ellipsoid parameters do not refine particularly well, and it was necessary to apply restraints to thermal and vibrational ellipsoid parameters of all atoms in order to achieve a sensible refinement. All C–H hydrogen atoms were inserted at geometric positions and ride on the attached atom. The O–H hydrogen atom on the  $\text{HSO}_4^-$  anion was inserted at an idealised hydrogen bonding position and rides on the attached atom.

SHELX-style weighting schemes struggled to deal with the data effectively, which we attribute to a combination of the weak data and the use of synchrotron radiation. Therefore, a quasi-unit weighting scheme was implemented. Analysis of the  $F_o/F_c$  plot showed that this handled the data better than a SHELX-style weighting scheme.

Generally this structure is of low quality, due to the weak data and the highly disordered hexyl chains. Nonetheless, the overall connectivity and anion binding location can be unambiguously determined.

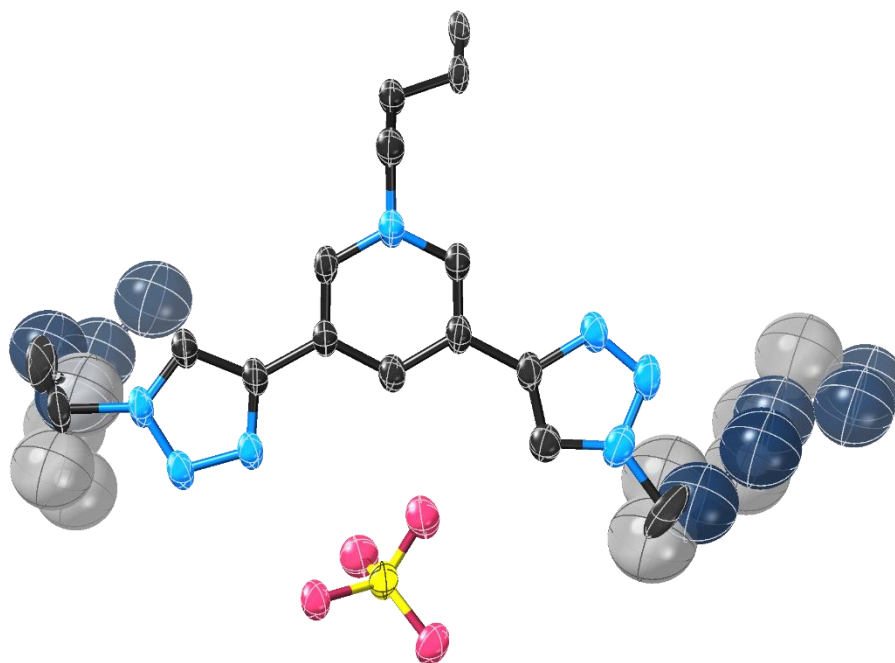


**Figure S56.** Thermal ellipsoid plot showing the asymmetric unit of  $2^{\text{H}}_{\text{hex}} \cdot (\text{HSO}_4)_2$ . Ellipsoids are shown at 50% probability, hydrogen atoms are omitted for clarity. PLATON-SQUEEZE<sup>S13</sup> was used. The two positions of the disordered hexyl chains are shown in grey and dark blue; these atoms were refined isotropically.

## $2^1_{\text{Bn}} \cdot (\text{HSO}_4)_2$

Crystals were small and weakly-diffracting and required the use of synchrotron radiation.

Refinement proceeded smoothly and no restraints were necessary. The  $\text{HSO}_4^-$  and methanol O-H proton were not visible in the Fourier difference map and so were inserted at idealised hydrogen bonding positions.

The  $\text{HSO}_4^-$  anion and methanol solvent form 1D hydrogen bonded chains with O...O separations of 2.59 and 2.91 Å. The  $\text{HSO}_4^-$  was assigned to the shorter O...O interaction, due to its greater acidity.

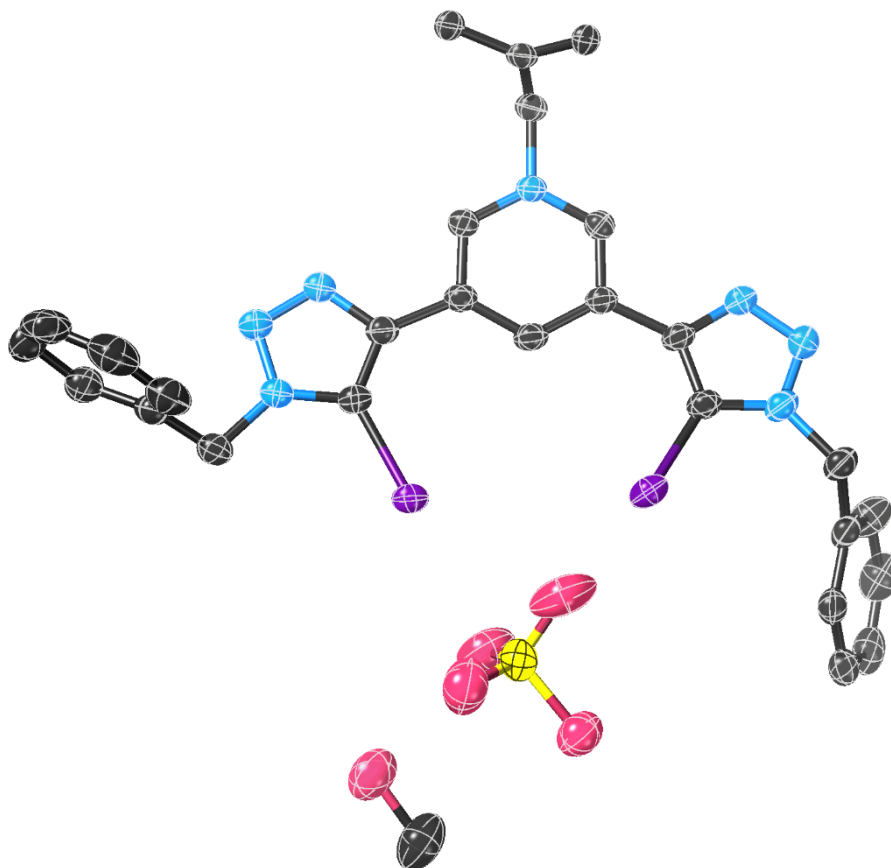


**Figure S57.** Thermal ellipsoid plot showing the asymmetric unit of  $2^1_{\text{Bn}} \cdot (\text{HSO}_4)_2$ . Ellipsoids are shown at 50% probability, hydrogen atoms are omitted for clarity.

### $2^1_{\text{Bn}} \cdot (\text{HSO}_4)_{1.2} \cdot \text{Br}_{0.8}$

The asymmetric unit contains half of the ditopic receptor, one anion site, and one methanol solvent molecule. The anion site refines well as a 0.6:0.4 mixture of  $\text{HSO}_4^- \cdot \text{Br}^-$ . We attribute the presence of  $\text{Br}^-$  to incomplete anion exchange in the previous step of the reaction converting  $2^1_{\text{Bn}} \cdot \text{Br}_2$  to  $2^1_{\text{Bn}} \cdot (\text{PF}_6)_2$  (see main text). The structure of  $2^1_{\text{Bn}} \cdot (\text{HSO}_4)_2$ , which was prepared from completely anion-exchanged  $2^1_{\text{Bn}} \cdot (\text{BF}_4)_2$  is very similar but contains only  $\text{HSO}_4^-$  anions.

C–H hydrogen atom positions were initially refined and then incorporated in a riding model. The exception was the three C–H hydrogen atoms on the methanol solvent, which did not refine sensibly and so were inserted at geometric positions and incorporated in a riding model. O–H hydrogen atom positions were inserted at idealised hydrogen bonding positions and then refined with restraints on bond lengths and bond angles.

Apart from restraints on hydrogen atom positions, it was not necessary to use any crystallographic restraints.

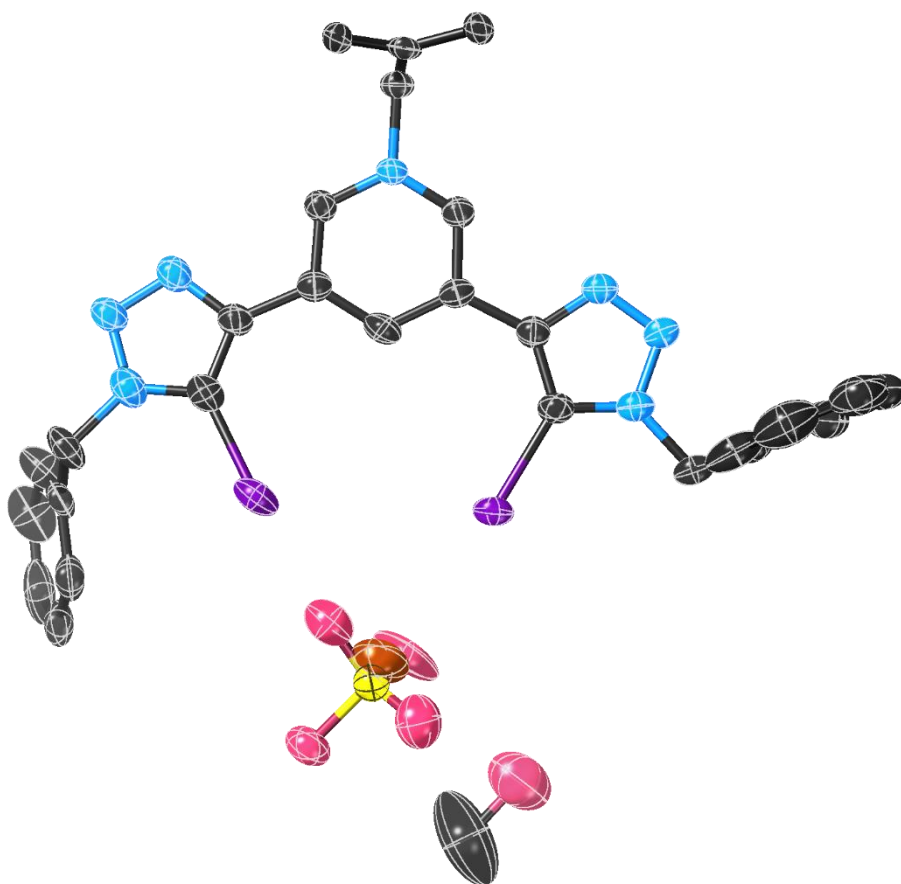


**Figure S58.** Thermal ellipsoid plot showing the asymmetric unit of  $2^1_{\text{Bn}} \cdot (\text{HSO}_4)_{1.2} \cdot \text{Br}_{0.8}$ . Ellipsoids are shown at 50% probability, hydrogen atoms are omitted for clarity.

## $2^1_{\text{Bn}}\cdot\text{Cl}_2$

Crystals were small and weakly diffracting and required the use of synchrotron radiation. The asymmetric unit contains half of a ditopic receptor, one chloride anion, and a half-occupancy water molecule.

O–H positions on the half-occupancy water molecule were inserted at idealised hydrogen bonding positions and ride on the attached oxygen atom. These hydrogen atom positions are relatively arbitrary.

It was necessary to apply restraints to the C–C bond lengths and thermal and vibrational ellipsoid parameters of one of the phenyl rings in order to achieve a chemically sensible refinement.

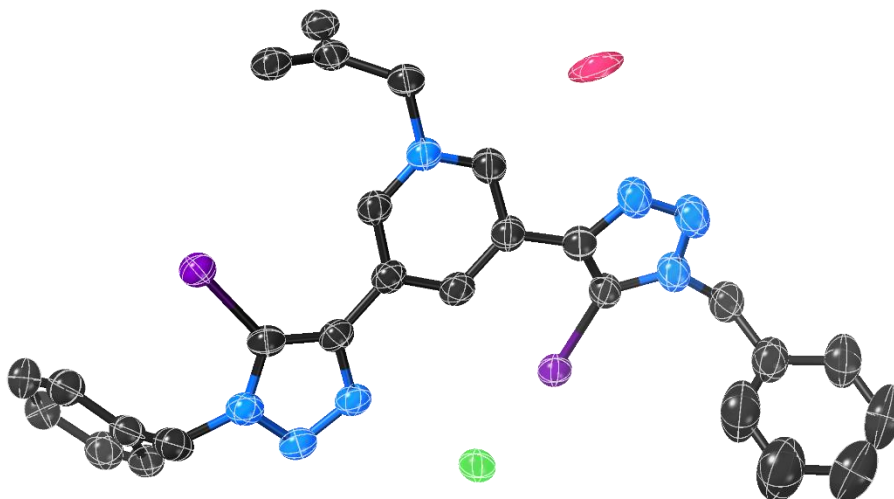


**Figure S59.** Thermal ellipsoid plot showing the asymmetric unit of  $2^1_{\text{Bn}}\cdot\text{Cl}_2$ . Ellipsoids are shown at 50% probability, hydrogen atoms are omitted for clarity.

**7<sup>H</sup>·Cl<sub>2</sub>**  
Crystals were small and weakly diffracting and required the use of synchrotron radiation. The asymmetric unit contains one ditopic receptor, two chloride anions, and one methanol solvent.

Hydrogen atoms were inserted using AFIX 43 commands. It was necessary to add DFIX restraints to the bond lengths of one of the pyridinium rings and SIMU restraints to two of the phenyl rings in order to achieve a chemically sensible refinement.

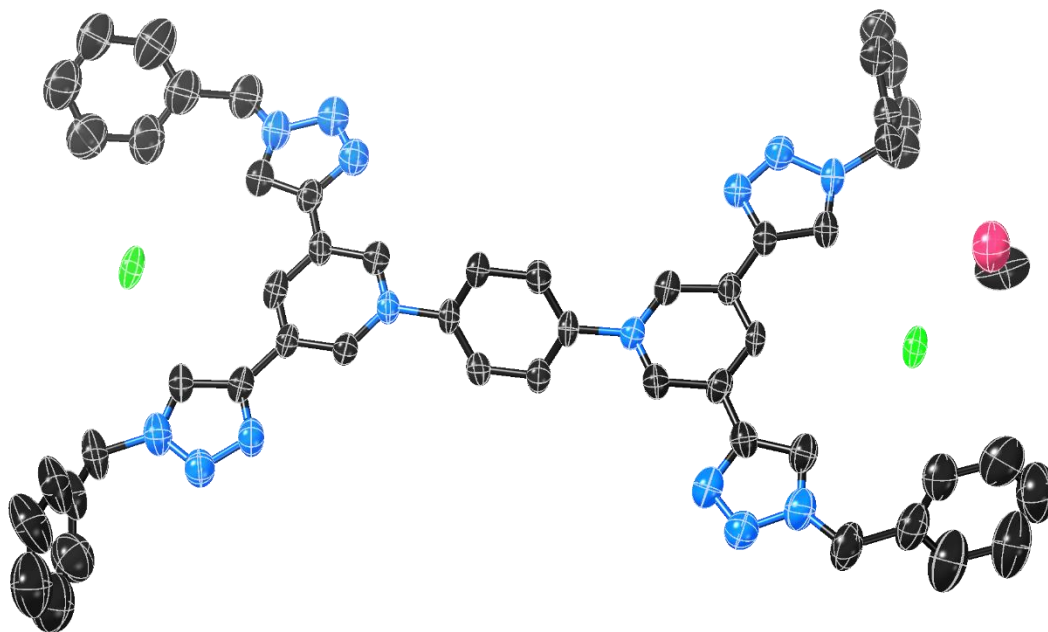


**Figure S60.** Thermal ellipsoid plot showing the asymmetric unit of 7<sup>H</sup>·Cl<sub>2</sub>. Ellipsoids are shown at 50% probability, hydrogen atoms are omitted for clarity.

### $8^{\text{H}}\cdot(\text{SO}_4)_2$

Crystals were tiny and very weakly diffracting and required the use of synchrotron radiation. Even using microfocus synchrotron radiation, no diffraction data could be obtained beyond 1.0 Å. Despite the very weak diffraction, the overall molecular architecture can be determined unambiguously.

Regions of diffuse electron density were present, presumably arising from disordered solvent molecules. It was not possible to model this electron density and so PLATON-SQUEEZE<sup>S13</sup> was used to include it in the refinement,

One of the sulfate anions is positionally disordered. This was modelled by having two positions for the four oxygen atoms (occupancies: 0.6:0.4). It was necessary to add restraints to the S–O bond lengths and O–S–O angles of this disordered anion as well as to the C–C bond lengths of some of the terminal phenyl groups in order to achieve a sensible refinement. Without the restraints on C–C bond lengths, the refinement was stable, but the phenyl ring bond lengths were not chemically sensible (ranging from 1.3 to 1.5 Å). Due to the low quality of the data, it was necessary to apply soft similarity restraints to thermal and vibrational ellipsoid parameters of all atoms.

C–H hydrogen atoms were inserted at calculated positions and ride on the attached carbon atom.

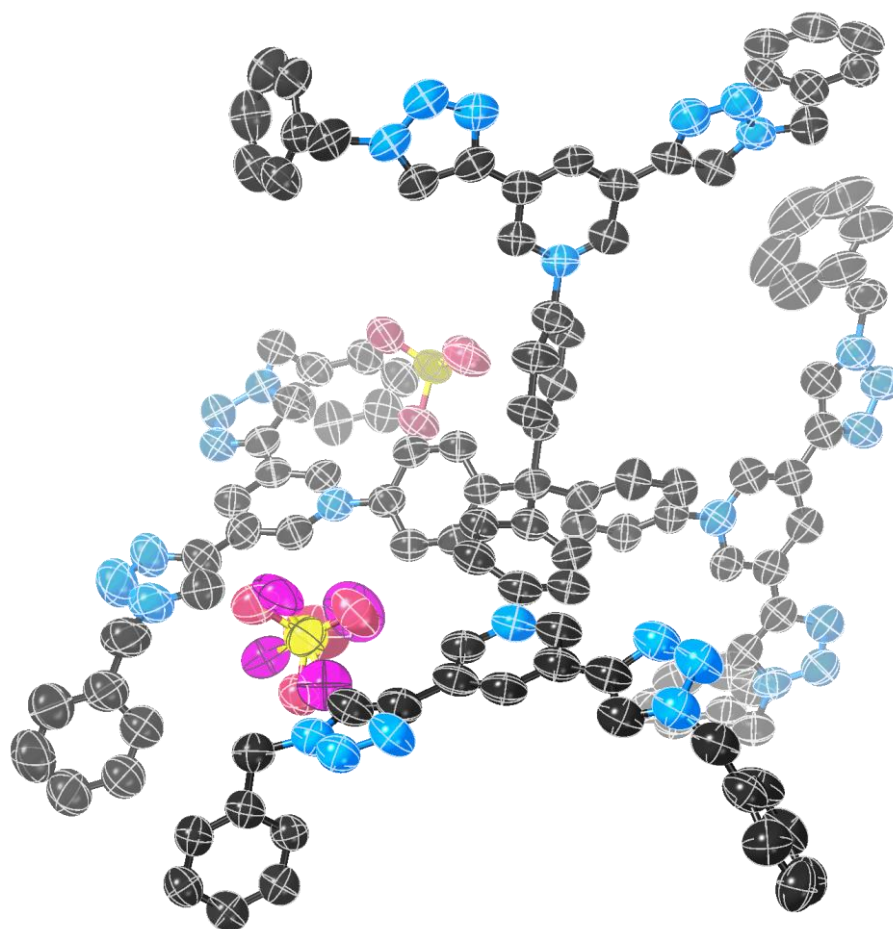


**Figure S61.** Thermal ellipsoid plot showing the asymmetric unit of  $8^{\text{H}}\cdot(\text{SO}_4)_2$ . Ellipsoids are shown at 50% probability, hydrogen atoms are omitted for clarity. PLATON-SQUEEZE<sup>S13</sup> was used. The two positions for the oxygen atoms of the disordered sulfate anion are shown in red and pink.

## Table of crystallographic data

**Table S1.** Selected crystallographic data.

Compound	1 <sup>H</sup> <sub>Bn</sub> <sup>a</sup>	2 <sup>H</sup> <sub>hex</sub> ·(HSO <sub>4</sub> ) <sub>2</sub> <sup>a,b</sup>	2 <sup>I</sup> <sub>Bn</sub> ·(HSO <sub>4</sub> ) <sub>2</sub>	2 <sup>I</sup> <sub>Bn</sub> ·(HSO <sub>4</sub> ) <sub>1.2</sub> Br <sub>0.8</sub>
Radiation type	Cu (λ = 1.54184 Å)	synchrotron (λ = 0.71090 Å)	synchrotron (λ = 0.71090 Å)	Mo (λ = 0.71073 Å)
Temperature (K)	150	100	100	150
Formula	C <sub>23</sub> H <sub>19</sub> N <sub>7</sub> · <i>solvents</i> <sup>a</sup>	C <sub>25</sub> H <sub>35</sub> N <sub>7</sub> ·HSO <sub>4</sub> · <i>solvents</i> <sup>a</sup>	(C <sub>54</sub> H <sub>42</sub> N <sub>14</sub> ) <sub>0.5</sub> ·HSO <sub>4</sub> ·CH <sub>4</sub> O	(C <sub>54</sub> H <sub>42</sub> N <sub>14</sub> ) <sub>0.5</sub> ·(HSO <sub>4</sub> ) <sub>1.2</sub> Br <sub>0.8</sub> ·CH <sub>4</sub> O
Formula weight	465.21	530.67	826.43	819.66
<i>a</i> (Å)	34.4367(18)	16.120(3)	13.546(3)	13.6171(5)
<i>b</i> (Å)	4.3516(2)	13.851(3)	18.552(3)	18.4028(6)
<i>c</i> (Å)	28.1754(15)	15.928(3)	12.799(2)	12.9206(6)
α (°)	90	90	90	90
β (°)	90	113.96(3)	114.375(10)	114.024(5)
γ (°)	90	90	90	90
Unit cell volume (Å <sup>3</sup> )	4222.2(4)	3249.8(14)	2929.8(2)	2933.9(2)
Crystal system	orthorhombic	monoclinic	monoclinic	monoclinic
Space group	<i>Pca</i> 2 <sub>1</sub>	<i>P</i> 2 <sub>1</sub> / <i>c</i>	<i>P</i> 2 <sub>1</sub> / <i>c</i>	<i>P</i> 2 <sub>1</sub> / <i>c</i>
<i>Z</i>	8	4	4	4
Reflections (all)	13159	23755	45444	34614
Reflections (unique)	6614	3050	6161	4887
<i>R</i> <sub>int</sub>	0.052	0.064	0.028	0.035
<i>R</i> <sub>1</sub> [ <i>I</i> > 2σ( <i>I</i> )]	0.084	0.135	0.064	0.068
<i>wR</i> <sub>2</sub> ( <i>F</i> <sup>2</sup> ) (all data)	0.241	0.240	0.166	0.145
CCDC number	2130560	2130563	2130561	2130562

<sup>a</sup> PLATON SQUEEZE<sup>S13</sup> was used. <sup>b</sup>This structure is of low quality.

Compound	2 <sup>I</sup> <sub>Bn</sub> ·Cl <sub>2</sub>	7 <sup>H</sup> ·Cl <sub>2</sub>	8 <sup>H</sup> ·(SO <sub>4</sub> ) <sub>2</sub> <sup>a,b</sup>
Radiation type	synchrotron (λ = 0.71075 Å)	synchrotron (λ = 0.71073 Å)	synchrotron (λ = 0.71075 Å)
Temperature (K)	100	100	100
Formula	C <sub>27</sub> H <sub>22</sub> N <sub>7</sub> Cl <sub>2</sub> ·(H <sub>2</sub> O) <sub>0.5</sub>	C <sub>52</sub> H <sub>42</sub> N <sub>14</sub> ·Cl <sub>2</sub> ·CH <sub>4</sub> O	C <sub>117</sub> H <sub>92</sub> N <sub>28</sub> ·(SO <sub>4</sub> ) <sub>2</sub> · <i>solvents</i> <sup>a</sup>
Formula weight	741.78	965.94	2082.34
<i>a</i> (Å)	16.037(3)	6.9910(4)	18.483(4)
<i>b</i> (Å)	20.726(4)	24.531(5)	18.604(4)
<i>c</i> (Å)	8.5250(17)	30.593(6)	18.986(4)
α (°)	90	90	87.77(4)
β (°)	101.95(3)	92.77(3)	61.09(3)
γ (°)	90	90	87.55(3)
Unit cell volume (Å <sup>3</sup> )	2772.10(3)	5240.4(18)	5708(3)
Crystal system	monoclinic	monoclinic	triclinic
Space group	<i>P</i> 2 <sub>1</sub> / <i>c</i>	<i>P</i> 2 <sub>1</sub> / <i>c</i>	<i>P</i> -1
<i>Z</i>	4	4	2
Reflections (all)	34758	35769	41245
Reflections (unique)	5603	5426	10392
<i>R</i> <sub>int</sub>	0.044	0.155	0.246
<i>R</i> <sub>1</sub> [ <i>I</i> > 2σ( <i>I</i> )]	0.040	0.083	0.110
<i>wR</i> <sub>2</sub> ( <i>F</i> <sup>2</sup> ) (all data)	0.122	0.258	0.363
CCDC number	2130565	2130564	2130566

<sup>a</sup> PLATON SQUEEZE<sup>S13</sup> was used. <sup>b</sup>This structure is of low quality.

## Cambridge Structural Database (CSD) searches

The Cambridge Structural Database,<sup>S15</sup> version 5.42 + three updates (most recent: September 2021) was searched for iodo-containing compounds having a “Non-Bonded Contact” between iodine and chloride in the range 1.93 and 3.86 Å (50–100% of the sum of the van der Waals radii<sup>S16</sup> of chlorine and iodine). Images of the search fragments used are provided in Figure S62. All identified structures were manually checked to see that the interaction was a chloride anion and not a negatively charged part of a larger anion such as PtCl<sub>4</sub><sup>2-</sup>. No quality filters (such as maximum values of R<sub>1</sub> were applied).

The lengths of these interactions are compared in Table S2. While the small number of samples mean that there is a limit to how much should be read into these data, it does seem apparent that iodoimidazolium and iodotriazolium form the shortest halogen bonds to chloride, while neutral iodoperfluoroarene and iodotriazole form longer bonds, and iodopyridinium groups are possibly longer again. Given the low number of samples and the fact that each functional group contains a range of structures (e.g. monodentate, bidentate), it was decided not to perform a statistical analysis of significance, although estimated standard errors of the means for contacts based on more than 10 structures were in the range 0.4–0.6%.

**Table S2.** Lengths of iodo⋯chloride interactions in the Cambridge Structural Database.

<i>charged halogen bonding motifs</i>					
	2-iodopyridinium	3-iodopyridinium	4-iodopyridinium	2-iodoimidazolium	4-iodotriazolium
Minimum	81	77	84	74	76
Maximum	81	87	84	81	78
Number	2	22	1	19	7
<b>Mean</b>	<b>81</b>	<b>83</b>	<b>84</b>	<b>78</b>	<b>77</b>
<i>neutral halogen bonding motifs</i>					
	iodoperfluoroarene		4-iodotriazole		
Minimum	77		78		
Maximum	85		86		
Number	22		16		
<b>Mean</b>	<b>81</b>		<b>81</b>		

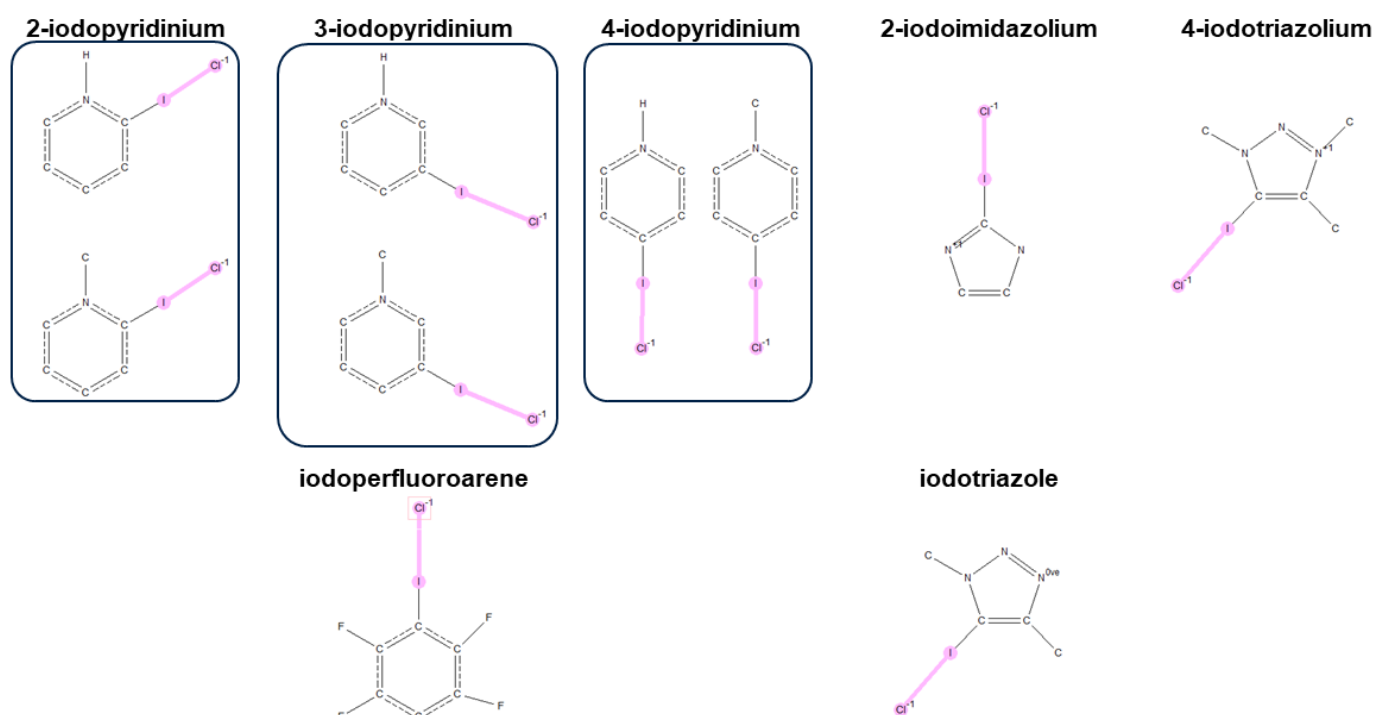


**Figure S62.** CSD search fragments used to obtain structures shown in Table S2. N<sup>+</sup>–H pyridinium and N<sup>+</sup>–C pyridinium structures (*i.e.* those in the boxes) were initially analysed separately, but found to be very similar and so were combined. The CSD was also searched for structures involving 2-iodoimidazole⋯Cl<sup>-</sup> interactions, but none were found.

## References

- <sup>S1</sup> H. E. Gottlieb, V. Kotlyar, A. Nudelman, NMR chemical shifts of common laboratory solvents as trace impurities, *J. Org. Chem.* **1997**, *62*, 7512–7515.
- <sup>S2</sup> E. Bosch, C. L. Barnes, Synthesis and crystallographic characterization of a novel platinocycle, *Organometallics*, **2000**, *19*, 5522–5524.
- <sup>S3</sup> J. Y. C. Lim, J. Y. Liew, P. D. Beer, Thermodynamics of anion binding by chalcogen bonding receptors, *Chem. Eur. J.* **2018**, *24*, 14560–14566.
- <sup>S4</sup> P. Wonner, A. Dreger, L. Vogel, E. Egnelage, S. M. Huber, Chalcogen bonding catalysis of a nitro-Michael reaction, *Angew. Chem. Int. Ed.*, **2019**, *58*, 16923–16927.
- <sup>S5</sup> *CrysAlis Pro*, **2011**, Oxford Diffraction.
- <sup>S6</sup> N. P. Cowieson, D. Aragao, M. Clift, D. J. Ericsson, C. Gee, S. J. Harrop, N. Mudie, S. Panjikar, J. R. Price, A. Riboldi-Tunnicliffe, R. Williamson, T. Caradoc-Davies, MX1: a bending-magnet crystallography beamline serving both chemical and macromolecular crystallography communities at the Australian Synchrotron, *J. Synchrotron Radiat.* **2015**, *22*, 187–190.
- <sup>S7</sup> D. Aragão, J. Aishima, H. Cherukuvada, R. Clarken, M. Clift, N. P. Cowieson, D. J. Ericsson, C. L. Gee, S. Macedo, N. Mudie, S. Panjikar, J. R. Price, A. Riboldi-Tunnicliffe, R. Rostan, R. Williamson, T. T. Caradoc-Davies, MX2: a high-flux undulator microfocus beamline serving both the chemical and macromolecular crystallography communities at the Australian Synchrotron, *J. Synchrotron Radiat.* **2018**, *25*, 885–891.
- <sup>S8</sup> W. Kabsch, *XDS*, *Acta Crystallogr.* **2010**, *D66*, 125–132.
- <sup>S9</sup> G. M. Sheldrick, *SHELXT* – Integrated space-group and crystal-structure determination, *Acta Crystallogr.* **2015**, *A71*, 3–8.
- <sup>S10</sup> L. Palatinus, G. Chapuis, *SUPERFLIP* – a computer program for the solution of crystal structures by charge flipping in arbitrary dimensions, *J. Appl. Crystallogr.* **2007**, *40*, 786–790.
- <sup>S11</sup> P. W. Betteridge, J. R. Carruthers, R. I. Cooper, K. Prout, D. J. Watkin, *CRYSTALS* version 12: software for guided crystal structure analysis, *J. Appl. Crystallogr.* **2003**, *36*, 1487.
- <sup>S12</sup> O. V. Dolomanov, L. J. Bourhis, R. J. Gildea, J. A. K. Howard, H. Puschmann, *OLEX2*: a complete structure solution, refinement and analysis program, *J. Appl. Crystallogr.* **2009**, *42*, 339–341.
- <sup>S13</sup> A. L. Spek, *PLATON SQUEEZE*: a tool for the calculation of the disordered solvent contribution to the calculated structure factors, *Acta Crystallogr.* **2015**, *A71*, 9–18.
- <sup>S14</sup> R. I. Cooper, A. L. Thompson, D. J. Watkin, *CRYSTALS* enhancements: dealing with hydrogen atoms in refinement, *J. Appl. Crystallogr.* **2010**, *43*, 1100–1107.
- <sup>S15</sup> R. Taylor, P. A. Wood, A million crystal structures: The whole is greater than the sum of its parts, *Chem. Rev.* **2019**, *119*, 9427–9477.
- <sup>S16</sup> S. Alvarez, A cartography of the van der Waals territories, *Dalton Trans.* **2013**, *42*, 8617–8636.